A model of whole plant gas exchange for herbaceous species from mountain grassland sites differing in land use

G. Wohlfahrt [a,b,*], M. Bahn [a], U. Tappeiner [a,c], A. Cernusca [a]

[a] *Institut für Botanik, Universität Innsbruck, Sternwartestr. 15, 6020 Innsbruck, Austria*
[b] *Centro di Ecologia Alpina, Viote del Monte Bondone, 38040 Trento, Italy*
[c] *Europäische Akademie Bozen, Domplatz 3, 39100 Bozen/Bolzano, Italy*

Abstract

A model is presented which aims at quantifying the CO_2 and H_2O gas exchange of whole plants in their natural microenvironment, the canopy. In an up-scaling approach the model combines leaf (gas exchange, energy balance) and canopy (radiative transfer, wind attenuation) scale simulations. Net photosynthesis and stomatal conductance are modelled using a nitrogen sensitive model of leaf gas exchange. An analytical solution to the energy balance equation is adopted to calculate leaf temperatures. Radiative transfer, separately for the wavebands of photosynthetically active, near-infrared and long-wave radiation, is simulated by means of a model which accounts for multiple scattering of radiation using detailed information on canopy structure as input data. Partial pressures of CO_2 and H_2O, as well as air temperatures within the canopy are not modelled, but instead, measured values are used as input data. Field studies were carried out at the ECOMONT pilot study area Monte Bondone (Trentino, Italy, 1550 m a.s.l.). The model is parametrised for four forbs and one graminoid species occurring at three sites differing in land use, i.e. an abandoned area, a meadow and a pasture. Independent measurements are used to validate each of the major submodels of the comprehensive whole plant gas exchange model. © 2000 Elsevier Science B.V. All rights reserved.

Keywords: Photosynthesis; Transpiration; Energy balance; Radiative transfer; Wind speed

1. Introduction

The gas exchange of plants in their natural microenvironment, the canopy, depends on the environmental driving forces of gas exchange, such as radiation, temperature and the partial pressures of CO_2 and H_2O, within the canopy, and the physiological potential of the individual leaves to respond to them (Schulze and Chapin, 1987; Barnes et al., 1990; Beyschlag et al., 1990; Baldocchi and Harley, 1995). Leaf physiology in turn is related to the long-term microclimatic conditions within the canopy. Adaptation to the gradient of photosynthetically active radiation is a

* Corresponding author. Tel.: + 43-512-507-5917; fax: + 43-512-507-2975.

E-mail address: georg.wohlfahrt@uibk.ac.at (G. Wohlfahrt)

well studied example (Hirose and Werger, 1987a,b; Chen et al., 1993; Hikosaka and Terashima, 1995, 1996; Anten and Werger, 1996). The driving forces of gas exchange within the canopy usually differ from those in the lower layer of the atmosphere (Oke, 1987; Monteith and Unsworth, 1990), depending on the degree of coupling between processes within and above canopy. Such coupling is determined by physical and physiological attributes of the vegetation itself, and by the state of the driving variables above the canopy (Jarvis and McNaughton, 1986; Oke, 1987; Baldocchi, 1992). Moreover, the microclimate within the canopy varies with canopy depth (Cernusca, 1977; Goudriaan, 1977; Cernusca and Seeber, 1981; Nobel, 1991; Baldocchi, 1992, 1993). Therefore the vertical position of leaf area plays a crucial role in determining the environmental driving variables actually experienced by the individual leaves, and thus their gas exchange (Caldwell et al., 1986; Barnes et al., 1990; Bahn et al., 1994; Anten and Werger, 1996).

This topic is best analysed by means of a model, which in the past has led to the emergence of a number of vegetation-atmosphere transfer models (Goudriaan, 1977; Caldwell et al., 1986; Tappeiner and Cernusca, 1991, 1998; Baldocchi and Harley, 1995; Leuning et al., 1995; Su et al., 1996; Baldocchi and Meyers, 1998). Given that the modellers' intention is to gain insights into the mechanisms governing gas exchange within the canopy, an up-scaling approach, using a multi-layer model, seems to be most appropriate (Norman, 1993; Leuning et al., 1995; Cernusca et al., 1998). Whereas top-down approaches, using so called big-leaf models, are probably the best choice for predictive purposes, especially at larger (e.g. regional) scales (Cernusca et al., 1998), where reduced accuracy (but see De Pury and Farquhar, 1997; Wang and Leuning, 1998; Boegh et al., 1999) is outweighed by computational efficiency (Sellers et al., 1992; Amthor, 1994; Kull and Jarvis, 1995; Lloyd et al., 1995; Tenhunen, 1999).

Up-scaling refers to the use of information at one spatial or temporal scale to infer characteristics on another scale (Norman, 1993). Scaling up gas exchange from leaves to the whole plant means, that information at the leaf level, i.e. leaf

area, leaf inclination, gas exchange characteristics, is combined with the environmental forces driving leaf gas exchange within the canopy, in order to quantify the fluxes of CO_2 and H_2O of whole plants (Wohlfahrt and Cernusca, 1999b). The modelling basis for such an up-scaling approach is a model of leaf level photosynthesis and stomatal conductance (Wohlfahrt and Cernusca, 1999a). This model is driven by the output of models, or alternatively, measured data, which describe the profiles of the environmental driving forces of gas exchange within the canopy. Summing up the predictions of net photosynthesis and transpiration, multiplied by the leaf area present in the various plant layers, then yields the CO_2 and H_2O gas exchange of whole plants (Wohlfahrt and Cernusca, 1999b).

The aim of this paper is to (i) present a model which meets the requirements for scaling up gas exchange from leaves to the whole plant; (ii) parameterise the model for five herbaceous species that grow at three sites differing in land use; and (iii) validate the various submodels of the comprehensive whole plant model using independent data sets.

2. Material and methods

2.1. Site and investigated plant species

Field investigations were carried out during the summers of 1996–1998 in the Southern Alps on the Monte Bondone plateau (Trentino/Italy, latitude 46°01′20″ N, longitude 11°02′30″ E) at an elevation between 1500–1600 m above sea level. The mean annual temperature is 5.5°C, ranging from −2.7°C in January to 14.4°C in July (Gandolfo and Sulli, 1993). Precipitation is abundant throughout the whole year (1189 mm), with two peaks in June (132 mm) and October (142 mm) and a minimum of 53 mm in January (Gandolfo and Sulli, 1993). Three sites, differing in land-use, were investigated: A hay meadow, mowed once a year, a pasture, grazed by cattle and horses, and an area abandoned 35 years ago. A general characterisation of the three sites is given in Table 1 and in Cescatti et al. (1999).

Criteria for the selection of the investigated species were that they should occur on all of the three sites and comprise a wide variety of different spatial strategies, i.e. differ with respect to the vertical positioning of their leaf area. Four forbs and one graminoid species were selected. *Nardus stricta* is a graminoid species characteristic for abandoned mountain grasslands, the remaining forbs, *Plantago atrata*, *Polygonum viviparum*, *Potentilla aurea* and *Trollius europaeus*, are equally abundant on the three study sites (Tasser et al., 1999). *P. atrata* and *N. stricta* exhibit a pyramidal leaf area distribution, the leaf area steadily declining from near the soil surface to the uppermost leaves, whereas *T. europaeus*, *P. aurea* and *P. viviparum* tend to display a proportionally larger amount of leaf area in the middle/upper layers. Among the latter three species *T. europaeus* is a strong competitor for light, as a result of its ability to overtop other species by elongating the petioles of the basal leaves, which make up most of the total leaf area (Bahn et al., 1994). Leaves of *P. aurea* and *P. viviparum* reach only about one third of the maximum height of the leaves of *T. europaeus*.

2.2. Experimental methods

Gas exchange measurements were carried out as described previously in detail by Wohlfahrt et al. (1998) and Bahn and Cernusca (1999). In brief, response curves to light and CO_2, which were used for the parameterisation of the photosynthesis model, were measured using two CO_2/H_2O porometers (Heinz WALZ GmbH., Effeltrich, Germany) along with the cuvettes PMK-10 and GK-0235P of the same origin, as well as a another fully climatised CO_2/H_2O porometer (CIRAS-1, PP-Systems, Hitchin Herts, UK). The latter was also used for episodical measurements of the diurnal course of photosynthesis and stomatal conductance under the prevailing environmental conditions and for measurements of leaf photosynthetic capacity (net photosynthesis at saturating PPFD, leaf temperature of 20°C and ambient CO_2 and H_2O partial pressures). The former data served to parameterise the stomatal conductance model, the latter were used to derive the nitrogen dependencies of the main photosynthetic component processes (Wohlfahrt et al., 1998; Wohlfahrt and Cernusca, 1999a). Calculations of net photosynthetic rate, stomatal conductance, transpiration rate and internal CO_2 partial pressure were made using the equations of Von Caemmerer and Farquhar (1981). All gas exchange rates are described on the basis of the projected leaf area, except for *N. stricta*, whose gas exchange rates are expressed on a surface area basis, because of its uniform circular leaf shape and its leaf orienta-

Table 1
General characterisation of the investigated sites at the Monte Bondone study area (From Cescatti et al., 1999)

	Meadow	Pasture	Abandoned area
Elevation (m a.s.l.)	1520	1565	1520
Exposition	E	E	SE
Inclination (°)	3	5	6
Management	Mowed	Grazed	Abandoned since 35 years
Vegetation type	Geranio-Trisetetum	Crepido-Cynosuretum	Siversio-Nardetum strictae
Maximum canopy height (cm)	80	16	30
Plant area index ($m^2 m^{-2}$)[a]	4.4 ± 0.6	4.5 ± 0.2	4.7
Leaf area index ($m^2 m^{-2}$)[a]	1.9 ± 0.9	2.3 ± 0.1	1.9
Mean leaf angle (°)[a]	58	34	57
Soil type	Cambisol with mull	Cambisol with mull	Cambisol with mull
Soil depth (cm)	75	42	60
Rooting depth (cm)[b]	20	13	20
Soil water storage capacity (mm)[b]	340	242	309

[a] Tappeiner and Sapinsky, unpublished.
[b] Neuwinger and Hofer, unpublished.

tion, which is more or less perpendicular to the ground surface (cf. Körner et al., 1979). Leaf area was measured using a leaf area meter (CI-203, CID Inc., Vancouver, USA). All measured leaves were collected, oven dried at 70°C for at least 72 h and weighed (AE-260, Mettler Instrumente AG, Greifensee-Zürich, Switzerland). Total leaf nitrogen was measured using an elemental analyser (CHNS-932, LECO Instruments, St. Joseph, USA).

Measurements of the micrometeorological parameters were made using the battery-powered data acquisition system MIKROMET (Cernusca, 1987) at time intervals ranging from 1 to 6 min. Hourly mean values were calculated. Incoming and reflected short-wave radiation was measured using star pyranometers, net radiation was measured by the means of net radiometers (Schenk, Vienna, Austria). Incoming photosynthetic photon flux density (PPFD) was measured using PAR-sensors (LI-190SA Quantum Sensor, Li-Cor, Lincoln, USA). One star pyranometer and one PAR-sensor had a shadow band in order to estimate the incoming diffuse radiation component. The profiles of PPFD within the canopy were measured using six ceptometers (SunScan, Delta-T-Devices LTD, Cambridge, UK) mounted at different heights within the canopy (see Fig. 6 for details). Leaf, soil and air temperatures were measured using thermocouples (copper/constantan, 0.08 mm diameter), CO_2 and H_2O pressures were measured using an infrared gas analyser (CIRAS-Sc, PP-Systems, Hitchin Herts, UK). Wind speed within the canopy was measured using thermo-electric anemometers (ThermoAir2, Schiltknecht, Gossau, Switzerland). Three-cup anemometers (Davis Instruments, Hayward, USA) were used to determine wind speed above the canopy.

Canopy structure was assessed at the time of the biomass maximum (end of July) by stratified clipping (Monsi and Saeki, 1953) of a square plot of 0.3–0.5 m lateral length. Thickness of the harvested layers ranged between 2 and 4 cm. Leaf area was determined by the means of a leaf area meter (LI-3100, Li-Cor, Lincoln, USA). The harvested plant material was separated by dominant species as well as by plant compartments (leaves,

stems, etc.; Tappeiner and Sapinsky, 1999). In this paper only the total plant area index (PAI) is used for the calculation of radiative transfer. Leaf and stem inclinations were measured in the field with a hand inclinometer with a five degrees accuracy (Tappeiner and Sapinsky, 1999).

Plant leaf architecture, again at the time of the biomass maximum, was recorded non-destructively on randomly selected individuals. Ten replicates per site and species were made (cf. Bahn et al., 1994; Bahn and Cernusca, 1999). Leaf area in each canopy layer was inferred from the products of maximum leaf length and width. Those products have been shown to correlate well with actual leaf area for a broad range of leaf sizes (Bahn et al., 1994; $R^2 > 0.93$ for the investigated species). Mean leaf inclinations for each plant layer were determined as described above.

Model performance was assessed with respect to both quantitative and qualitative correspondence to measured data (cf. Pachepsky et al., 1996). The Pearson's correlation coefficient and the *F*-test were used in order to test whether the different submodels are quantitatively adequate. Qualitative model performance was evaluated by analysing the residuals, which were calculated as the difference between predicted and observed values, and deviations from 1:1 correspondence in the *y*-intercept and the slope obtained from linear regression analysis of observed versus predicted values.

2.3. Models

In the present study, a one-dimensional, multi-layer model is used to compute the fluxes of CO_2 and H_2O of whole plants (Wohlfahrt and Cernusca (1999b). The model combines calculations at the canopy and the whole plant level. It consists of coupled micrometeorological and physiological modules, as depicted in Fig. 1. The micrometeorological modules compute radiative transfer (separately for the PPFD, near-infrared (NIR) and long-wave radiation), the attenuation of wind speed at the canopy level and leaf temperatures at the whole plant level. The profiles of CO_2, H_2O and air temperature within the canopy are not modelled, but instead, measured values
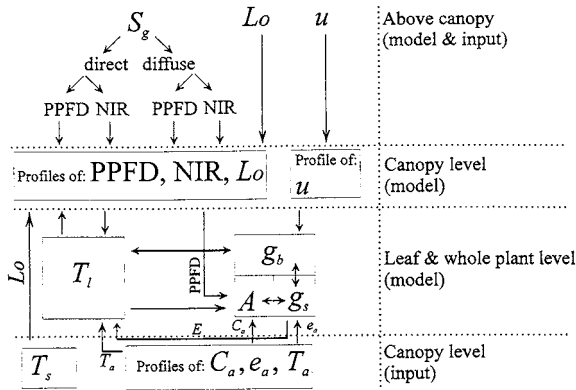
Fig. 1. Conceptual diagram showing the main submodels of the comprehensive whole plant gas exchange model and their interdependence. For symbols and abbreviations refer to Appendix C.

used as input data (Fig. 1). The environmental variables computed in the micrometeorological modules represent the driving forces for the leaf gas exchange model, which calculates net photosynthesis, stomatal conductance and transpiration at the whole plant level. Since the long-wave radiation emitted by leaves depends upon leaf temperature, but in turn determines leaf temperature via the leaf energy balance, an iterative procedure is used to find equilibrium states. For symbols and abbreviations refer to Appendix C.

2.3.1. Leaf gas exchange

The model of leaf gas exchange has been described in detail by Wohlfahrt et al. (1998), the corresponding model theory is therefore not repeated in the present paper.

2.3.2. Leaf boundary layer conductance

In the case of forced convection (and assuming a laminar flow of air over the leaf surface) the single-sided leaf boundary layer conductance to water vapour (g_{bvf}) is given by (Campbell and Norman, 1998)

$$g_{bvf} = \frac{1}{2} \cdot 1.4 \cdot 147 \cdot \sqrt{\frac{u}{w}} \tag{1}$$

where the factor $\frac{1}{2}$ converts two-sided to single-sided values for broad leaves (Nikolov et al., 1995) and 1.4 accounts for the enhancement of

the boundary layer conductance as a result of the turbulent nature of wind in outdoor environments (Campbell and Norman, 1998); u is the wind speed and w is the characteristic leaf dimension, which was approximated by taking the leaf width. At low wind speeds, the heat exchange is dominated by free convection and the single-sided leaf boundary layer conductance to water vapour (g_{bve}), assuming laminar free convection, may be found as (Campbell and Norman, 1998)

$$g_{bve} = \frac{1}{2} \cdot 55 \cdot \left(\frac{|T_1 - T_a|}{w} \right)^{1/4} \tag{2}$$

where T_1 and T_a are the leaf and air temperatures, respectively. The final single-sided leaf boundary layer conductance to water vapour (g_{bv}) is the larger of the conductances resulting from forced and free convective exchanges (Nikolov et al., 1995). Conductances may be converted from units of mmol m^2 s^{-1} to m s^{-1} by (Nikolov et al., 1995)

$$c_{fm} = 8.309 \cdot 10^{-5} \cdot \frac{T_{ak}}{P}, \tag{3}$$

where T_{ak} is the absolute air temperature and P is the air pressure at the study site. The CO_2 and H_2O partial pressures within the boundary layer differ from those in the air surrounding the leaf, depending on the respective partial pressures in the leaf intercellular space (C_i and $e_s (T_1)$) and the air outside the leaf boundary layer (C_a and e_a), as well as the stomatal (g_{sv}) and boundary layer conductances for the respective species. According to Falge (1997) the relative humidity, h_s, and the CO_2 partial pressure, C_s, in the leaf boundary layer may be found as

$$h_s = \frac{e_a}{e_s(T_1)} - \frac{1}{1 + \dfrac{g_{bv}}{g_{sv}}} \cdot \frac{e_a - e_s(T_1)}{e_s(T_1)}, \tag{4}$$

$$C_s = C_a - \frac{1.37}{1.37 + \dfrac{1.6 \cdot g_{bv}}{g_{sv}}} \cdot (C_a - C_i). \tag{5}$$

The factors 1.6 and 1.37 account for the difference in the diffusivity of CO_2 and H_2O in air and the boundary layer, respectively (Farquhar and Sharkey, 1982).

2.3.3. Leaf energy balance

Leaf temperatures were estimated solving their energy balance equation (Campbell and Norman, 1998)

$$
\begin{aligned}
R_{abs} &= L_{oe} + \lambda E + H \\
&= 2 \cdot \varepsilon_l \cdot \sigma \cdot T_{lk}^4 + \frac{\rho \cdot c_p}{\gamma} \cdot [e_s(T_l) - e_a] \cdot g_{tv} \\
&\quad + \rho \cdot c_p \cdot (T_l - T_a) \cdot 2 \cdot 0.924 \cdot g_{bv},
\end{aligned} \tag{6}
$$

where R_{abs} is the bi-directional absorbed short-wave and long-wave radiation, Lo_e is the emitted long-wave radiation, λE and H represent latent and sensible heat losses, respectively; ε_l is the leaf thermal emissivity, σ is the Stefan-Boltzmann constant, ρ and c_p are the density and the specific heat of dry air, respectively, γ is the psychrometric constant and g_{tv} the leaf total conductance to water vapour. Energy losses as a result of emitted long-wave radiation and sensible heat occur from both the upper and lower leaf surface, which is accounted for by the factor 2. The boundary layer conductance to water vapour (g_{bv}) is converted to that for heat by the factor 0.924 (Nikolov et al., 1995). The density of dry air is estimated from (Smithsonian Meteorological Tables)

$$
\rho = 3.4838 \cdot 10^{-1} \cdot \frac{P}{T_{ak}} \tag{7}
$$

and the psychrometric constant is given by

$$
\gamma = \frac{P \cdot c_p}{6.22 \cdot 10^{-3} \cdot L}, \tag{8}
$$

where L is the latent heat of vaporization, which is given by (Verstraete, 1985)

$$
L = (2.50084 - 0.00234 \cdot T_a) \cdot 10^6. \tag{9}
$$

The leaf total conductance to water vapour (for a dry leaf surface) is given by

$$
g_{tv} = \frac{g_{sv} \cdot g_{bv}}{g_{sv} + g_{bv}}. \tag{10}
$$

The leaf saturation vapour pressure may be described using the Tetens formula (Buck, 1981)

$$
e_s(T_l) = 6.107 \cdot \exp\left(\frac{17.502 \cdot T_l}{T_l + 240.97}\right), \tag{11}
$$

or may be approximated by a fourth-order polynomial over the temperature range from -5 to 60°C,

with a maximum error of 0.48% at -2°C (Nikolov et al., 1995)

$$
\begin{aligned}
e_s(T_l) &= 5.82436 \cdot 10^{-6} \cdot T_l^4 + 1.5842 \cdot 10^{-4} \cdot T_l^3 \\
&\quad + 1.55186 \cdot 10^{-2} \cdot T_l^2 + 44.513596 \cdot 10^{-2} \cdot T_l \\
&\quad + 6.079. \tag{12}
\end{aligned}
$$

The use of Eq. (12) allows for an analytical solution to the energy balance equation for leaf temperature as proposed by Paw U (1987), by arranging Eq. (6) in the form of a quartic equation as described in Appendix A.

2.3.4. Wind profile

The bi-layered structure of the investigated canopies, consisting of two distinct layers, a lower, much denser one, dominated by forbs and an upper, sparser one, composed almost exclusively by erect stems and leaves of the occurring graminoid species (Tappeiner and Cernusca, 1994), made it necessary to apply two different equations in order to describe the wind profile within the investigated canopies (Cernusca, 1977). The attenuation of wind speed above the canopy, but also within the canopy down to the upper boundary formed by the forbs, termed h, was described applying a logarithmic wind law. The attenuation below h was described using an exponential equation (Goudriaan, 1977; Campbell and Norman, 1998)

$$
u(z) = \frac{u^*}{0.4} \cdot \ln \frac{z - d}{z_0} \quad \text{if } z > h, \tag{13}
$$

$$
u(z) = u(h) \cdot \exp\left[a \cdot \left(\frac{z}{h} - 1\right)\right] \quad \text{if } z \leq h. \tag{14}
$$

Where u^* is the friction velocity, z is the canopy height, d is the zero plane displacement, z_0 is the momentum roughness parameter and a is an extinction coefficient (Campbell and Norman, 1998).

2.3.5. Radiative transfer

Radiative transfer was modelled adopting the basic equations by Goudriaan (1977). The canopy is divided into sufficiently small (PAI = 0.1 m^2 m^{-2}) layers with negligible self-shading, in which leaves are assumed to be distributed symmetrically with respect to the azimuth. The model accounts

for multiple scattering of radiation, assuming leaf reflection and transmission to be lambertian and of equal magnitude, and considers nine leaf angle classes (λ).

The probability that a ray of light incident at an angle (from the horizontal) β' is intercepted in a layer of leaves with a PAI of ΔL, inclined as described by a leaf angle distribution F and distributed in space according to a leaf clumping factor Ω, is given by (Nilson, 1971; Goudriaan, 1977; Baldocchi and Collineau, 1994)

$$M_i(j, \beta') = \frac{\Omega(j) \cdot \Delta L(j)}{\sin \beta'} \cdot \sum_{\lambda = 1}^{9} F(j, \lambda) \cdot O(\beta', \lambda), \tag{15}$$

where j is the index of the canopy layer counted from bottom upwards. Ω is a leaf clumping factor, being equal to one when leaves are distributed randomly, smaller than one when leaves are clumped and larger than one when leaves are distributed uniformly (Goudriaan and Van Laar, 1994; Campbell and Norman, 1998). $O(\beta', \lambda)$ is the projection of a leaf inclined at an angle λ into the direction β' (De Wit, 1965; Ross, 1975, 1981; Goudriaan, 1977, 1988), which may be calculated as

$$O(\beta', \lambda) = \sin \beta' \cdot \cos \lambda \quad \text{if} \quad \beta' \geq \lambda \tag{16}$$

$$O(\beta', \lambda)$$
$$= \frac{2}{\pi} \cdot \left[\sin \beta' \cdot \cos \lambda \cdot \arcsin\left(\frac{\tan \beta'}{\tan \lambda}\right) \right.$$
$$\left. + \sqrt{\sin^2 \lambda - \sin^2 \beta'} \right] \quad \text{if} \quad \beta' < \lambda. \tag{17}$$

The fraction of light not intercepted in a layer, M_t (j, β'), is simply given as $1 - M_i$ (j, β'). For the treatment of diffuse radiation, the upper and lower hemispheres viewed by leaves are divided into 9 classes of 10 degrees each, which are referred to as β', in contrary to β, which refers to the inclination of the sun. The downward (Q_d) and upward (Q_u) fluxes within the canopy consist of the non-intercepted radiation from above and below (first part on the right hand side of Eqs. (18) and (19)), respectively, and the part of the intercepted radiation which is scattered in the downward and upward direction (second part on the right hand side of Eqs. (18) and (19)), respectively, as

$$Q_d(j, \beta') = M_t(j, \beta') \cdot Q_d(j + 1, \beta')$$
$$+ 0.5 \cdot \chi_1 \cdot B_l(j, \beta') \cdot Q_i(j) \tag{18}$$

$$Q_u(j, \beta') = M_t(j, \beta') \cdot Q_u(j - 1, \beta')$$
$$+ 0.5 \cdot \chi_1 \cdot B_l(j, \beta') \cdot Q_i(j). \tag{19}$$

Where χ_1 is a wavelength-dependent leaf scattering coefficient, B_l is a view factor and the factor 0.5 arises from equal reflection and transmission by the leaves. Q_i is the light intercepted in a layer, which is given as

$$Q_i(j)$$
$$= \sum_{\beta' = 1}^{9} [Q_d(j + 1, \beta') + Q_u(j - 1, \beta')] \cdot M_i(j, \beta'). \tag{20}$$

The view factor, B_l, is given by

$$B_l(j, \beta') = \frac{B_u(\beta') \cdot M_i(j, \beta')}{\sum_{\beta' = 1}^{9} B_u(\beta') \cdot M_i(j, \beta')}, \tag{21}$$

where B_u represents the weights according to the Uniform Overcast Sky (UOC; Goudriaan, 1977). At the soil surface, the lower boundary condition of the model, light is reflected lambertian according to the UOC as

$$Q_u(0, \beta') = \chi_s \cdot B_u(\beta') \cdot \sum_{\beta' = 1}^{9} Q_d(1, \beta'), \tag{22}$$

where χ_s is a wavelength-dependent soil scattering coefficient. The equations so far, using the appropriate above canopy radiation values and soil/leaf scattering coefficients, apply for solar radiation, i.e. the PPFD and NIR wavebands. For long-wave radiation, Eqs. (18)–(20) and (22) have to be modified to account for two additional radiation fluxes. These result from the fact that both leaves and the soil emit thermal radiation, depending on their absolute temperature (Stefan-Boltzmann law). Thus for the downward and upward fluxes of long-wave radiation Eqs. (18) and (19) have to be modified as

$$L_{o_d}(j, \beta') = M_t(j, \beta') \cdot L_{o_d}(j + 1, \beta')$$
$$+ \chi_1 \cdot B_l(j, \beta') \cdot \sum_{\beta' = 1}^{9} M_i(j, \lambda)$$
$$\cdot L_{o_u}(j - 1, \beta') + \varepsilon_1 \cdot B_l(j, \beta') \cdot B_u(\beta')$$
$$\cdot \sigma \cdot [T_{lksl}(j)^4 \cdot f_{sl} + T_{lksh}(j)^4 \cdot (1 - f_{sl})] \tag{23}$$

$$L_{o_u}(j, \beta') = M_t(j, \beta') \cdot L_{o_u}(j - 1, \beta')$$
$$+ \chi_1 \cdot B_1(j, \beta') \cdot \sum_{\beta'=1}^{9} M_i(j, \lambda)$$
$$\cdot L_{o_d}(j + 1, \beta')$$
$$+ \varepsilon_1 \cdot B_1(j, \beta') \cdot B_u(\beta') \cdot \sigma \cdot [T_{lksl}(j)^4 \cdot f_{sl}$$
$$+ T_{lksh}(j)^4 \cdot (1 - f_{sl})] \tag{24}$$

The leaf emitted long-wave radiation, which is assumed to be distributed isotropically, is calculated as the weighted mean flux from sunlit and shaded leaves, which radiate at an absolute temperature T_{lksl} and T_{lksh}, respectively, where f_{sl} is the fraction of sunlit leaf area (see below). Since leaves do not transmit long-wave radiation χ_1 is not a scattering coefficient, but refers to reflection of long-wave radiation only. The equation describing the reflection of the long-wave radiation flux at the soil surface has to account for the soil emitted long-wave radiation according to

$$L_{o_u}(0, \beta') = B_u(\beta')$$
$$\cdot \left[\varepsilon_s \cdot \sigma \cdot T_{sk}^4 + \chi_s \cdot \sum_{\beta'=1}^{9} L_{o_d}(1, \beta') \right], \tag{25}$$

where ε_s and χ_s are the soil emissivity and reflection coefficients, respectively, and T_{sk} is the absolute soil surface temperature. The soil and the sky emitted long-wave radiation represent state variables and thus the corresponding canopy profiles are calculated only once per time step. In most cases time steps are half-hourly or hourly (cf. Nikolov et al., 1995), but may be kept flexible to match input data. Whereas the profile of long-wave radiation emitted by leaves depends upon leaf temperatures and in turn influences leaf temperatures via the energy balance (Eq. (6)), making it necessary to solve in an iterative fashion for the equilibrium leaf temperatures.

A relaxation method, by which the scattered fluxes are added to the fluxes already there, was applied to solve for Eqs. (18), (19) and (22)–(25), as described in Goudriaan (1977). A maximum number of five runs was necessary to reach convergence for the NIR, two were needed for the PPFD and long-wave radiation. The model thus accounts for fifth-order scattering in the NIR waveband and for second-order scattering in the PPFD and long-wave wavebands.

Now that the radiation field within the canopy has been specified, it is possible to calculate the amount of radiation intercepted and/or absorbed by the leaves of the plants. Because of the non-linear response of photosynthesis to PPFD the radiation incident on shaded and sunlit leaves must be considered separately (Spitters, 1986). Shaded leaves receive diffuse light only (Q_{shade}, Eq. (27)), while sunlit leaves receive both diffuse and direct radiation (Q_{sun}, Eq. (28)), the latter incident at an angle β, the elevation of the sun. The flux of diffuse radiation in the canopy consists of diffuse radiation from the sky and of diffused, scattered beam radiation. Thus to obtain the radiation incident on shaded leaves the direct component (Q_{dir}), whose attenuation is calculated as

$$Q_{dir}(j) = Q_{dir}(j + 1) \cdot M_t(j, \beta), \tag{26}$$

has to be subtracted from total radiation

$$Q_{shade}(jp)$$
$$= \left\{ \sum_{\beta'=1}^{9} \left[\frac{O(\beta', \lambda_p)}{\sin \beta'} \cdot (Q_{down}(j + 1, \beta) \right. \right.$$
$$\left. \left. + Q_{up}(j - 1, \beta')) \right] \right\} - Q_{dir}(j + 1) \cdot \frac{O(\beta, \lambda_p)}{\sin \beta}, \tag{27}$$

where the index p indicates whole plant values. The radiation incident on sunlit leaves may then be calculated as

$$Q_{sun}(jp) = Q_{shade}(jp) + Q_{dir}(n + 1) \cdot \frac{O(\beta, \lambda_p)}{\sin \beta} \tag{28}$$

where $Q_{dir}(n + 1)$ stands for the direct radiation measured on a horizontal plane above the canopy. In the present approach average leaf angles are used for the different plant layers (λ_p). If a leaf angle distribution was to be used instead, O in Eqs. (27), (28) and (30) needs to be calculated as the weighted average over the different leaf angle classes, as in Eq. (15). The fraction of leaves which receive both direct and diffuse radiation, i.e. the fraction of sunlit leaves f_{sl}, is given by

$$f_{sl}(j) = f_{sl}(j + 1) \cdot M_I(j, \beta). \tag{29}$$

The results of Eqs. (27) and (28) may be used directly to calculate assimilation, because PPFD in the leaf model (Eq. (6) in Wohlfahrt et al., 1998) refers to an incident light basis. In order to calculate absorbed short-wave radiation, as it is required for the leaf energy balance (Eq. (6)), Q_{shade} and Q_{sun} need to be multiplied by an absorption coefficient, which is calculated as $1 - \chi_l$. The long-wave radiation absorbed by both sunlit and shaded leaves is given by

$$L_o(jp) = \sum_{\beta'=1}^{9} \left[\frac{O(\beta, \lambda_p)}{\sin \beta'} \cdot (L_{o_d}(j+1, \beta') + L_{o_u}(j-1, \beta')) \cdot (1 - \chi') \right]. \quad (30)$$

Solar geometry, determining the position of the sun in the sky, was calculated using the equations given in Campbell and Norman (1998). Total solar radiation, as well as the partitioning of solar radiation into direct and diffuse, PPFD and NIR components, is either modelled using the approach described in Goudriaan (1977) and Goudriaan and Van Laar (1994), or measured values (as described in a previous section) are used instead. Similarly sky long-wave radiation may be either estimated using the equations by Brutsaert (1984) and Monteith and Unsworth (1990), or measured values be used. Details on the corresponding algorithms are given in Appendix B.

3. Results and discussion

3.1. Parameterisation

3.1.1. Leaf gas exchange

The parameterisation of the gas exchange models of the investigated species was the topic of a previous paper (Wohlfahrt et al., 1998), and therefore will not be discussed in detail. In brief, estimates of R_{dark}, the dark respiration rate, were made from the y-intercept of linear regressions describing the initial portion of light response curves at different temperatures. V_{cmax} and P_{ml}, the maximum rate of carboxylation and the potential rate of RuBP regeneration, were inferred from A/C_i curves at different temperatures using

non-linear least-squares regression technique to Eq. (1) from Wohlfahrt et al. (1998), as described also by Harley et al. (1992), Wullschleger (1993) and Walcroft et al. (1997a). Temperature dependent parameters describing V_{cmax}, P_{ml} and R_{dark} were then obtained by fitting Eqs. (7) and (8) from Wohlfahrt et al. (1998) to these values, again using non-linear least-squares regression technique (Table 2A). Parameters describing the nitrogen dependency of V_{cmax}, C_N and C_0 (Table 2A), were derived from linear regressions relating V_{cmax}, which was calculated from photosynthesis at ambient CO_2 partial pressure and saturating light intensity, to leaf nitrogen content. Parameters of the stomatal conductance model, G_{fac} and g_{min} (Table 2B), were derived from the slope and the y-intercept, respectively, of a linear regression through the data points of the product of $(A + I_{fac} \cdot R_{dark}) \cdot 10^2 \cdot h_s \cdot C_s^{-1}$ plotted against measured stomatal conductance, g_{sv} (Ball et al., 1987). Water availability has been shown to influence the parameters of the stomatal conductance model (Sala and Tenhunen, 1996; Baldocchi, 1997). This was accounted for by determining G_{fac} and g_{min} separately for each site (Table 2B). Finally α, the apparent quantum yield at saturating CO_2 partial pressure, was adjusted to give a good fit to the initial portion of the light response curves (Table 2A). Parameters determining the temperature dependency of the RUBISCO specificity factor were taken from Jordan and Ogren (1984), those of the Michaelis–Menten constants for carboxylation and oxygenation from Badger and Collatz (1977). Since upper leaves ($> 12–16$ cm) of $T.$ $europaeus$ showed visible signs of senescence already during June, when the lower leaves were fully developed, we parameterised them separately.

3.1.2. Wind profile

Measurements of wind speed above h, the height of the lower canopy layer dominated by forbs (Fig. 2), were fitted to Eq. (13) by non-linear least-squares regression technique, yielding parameter estimates for u^* and z_m. In this procedure d was fixed at approx. $0.65 \cdot h$ (Table 3), which has been shown to be in good agreement with the results of several studies by Campbell and Norman (1998). The values obtained for z_m (Table 3), a measure for the aerodynamic rough

ness of the canopy surface (Oke, 1987), are close to $0.1 \cdot h$, which has been proposed as a good approximation for z_m by several authors (Maki 1975; Nobel, 1991; Campbell and Norman, 1998). The extinction coefficient for wind speed, a, was estimated by fitting measurements of wind speed below h (Fig. 2) to Eq. (14) by the means of non-linear least-squares regression technique. The values shown in Table 3 are in good agreement with a range for a between 1–3, reported by Cionco (1972), Goudriaan (1977) and Pereira and Shaw (1980) for grass and crop canopies of similar PAI. There is little difference in values of a between the meadow and the abandoned area, whereas the value for the pasture is considerably lower. This reflects the sharp decrease of wind speed in the dense canopy layers below h at the pasture (Fig. 2). Goudriaan (1977) suggests a simple method for calculating values of a as a function of canopy structure, namely the total PAI, canopy height and average leaf width. Applying this equation using an average leaf width of 0.02 m to the investigated canopies, yields estimates for a of 2.5, 2.8 and 1.7 for the abandoned area, the meadow and the pasture, respectively. Though not exactly matching a derived from measured wind speeds (Table 3), the similarity of the values, as well of the relative differences between the three canopies is striking, confirming the estimates of a in Table 3 and the validity of the approach of Goudriaan (1977) for determining a of mountain grassland canopies. At a given canopy height, wind speeds are highest at the pasture, followed by the abandoned area and the meadow, thus being inversely dependent on h (Fig. 2 and Table 3).

Table 2

Parameters of the combined photosynthesis (A) and stomatal conductance (B) model (from Wohlfahrt et al., 1998) for *N. stricta* (Nast), *P. atrata* (Plat), *P. viviparum* (Povi), *P. aurea* (Poau) and lower (lo) and upper (up) leaves of *T. europaeus* (Treu)[a]

Parameter		Units	Nast	Plat	Povi	Poau	Treu$_{lo}$	Treu$_{up}$
(A)								
V_{cmax}	$\Delta H_a(V_{cmax})$	J mol^{-1}	61 304	64 490	60 940	57 098	68 000	68 362
	$\Delta H_a(V_{cmax})$	J mol^{-1}	202 583	20 0000	199 571	204 000	201 000	202 198
P_{ml}	$\Delta H_a(P_{ml})$	J mol^{-1}	44 386	51 014	61 521	57 101	55 465	55 465
	$\Delta H_a(P_{ml})$	J mol^{-1}	196 168	19 7551	192 521	199 247	199 521	199 521
R_{dark}	$\Delta H_a(R_{dark})$	J mol^{-1}	13 592	53 132	17 913	94 482	36 743	37 246
	α	mol CO_2 mol photons^{-1}	0.05	0.05	0.06	0.06	0.06	0.045
$V_{cmax}(T_{ref})$	C_N	µmol CO_2 mmol^{-1} N s^{-1}	0.481	0.369	0.617	0.530	0.287	0.423
	C_0	µmol m^{-2} s^{-1}	−9.87	14.81	−39.52	−18.42	3.94	−22.86
	R_{fac}	–	0.054	0.031	0.076	0.023	0.037	0.055
	P_{fac}	–	0.649	0.600	0.661	0.580	0.665	0.638
Parameter	Units	Site						
(B)								
G_{fac}	–	A	16.0	9.8	12.0	24.7	12.8	20.2
		M	16.0	13.8	11.9	17.0	13.4	19.2
		P	16.0	14.1	8.9	10.6	9.1	9.4
g_{min}	mmol m^{-2} s^{-1}	A	21.9	76.1	54.5	130.0	70.6	94.7
		M	21.9	70.0	57.0	120.0	67.0	29.5
		P	21.9	79.3	41.2	74.6	81.5	32.7

[a] For abbreviations and symbols refer to Appendix C (A, abandoned area; M, meadow; P, pasture). $\Delta S(V_{cmax})$ and $\Delta S(P_{ml})$ were fixed for all species at 656 and 643 J K^{-1} mol^{-1}, respectively (cf. Wohlfahrt et al., 1998).
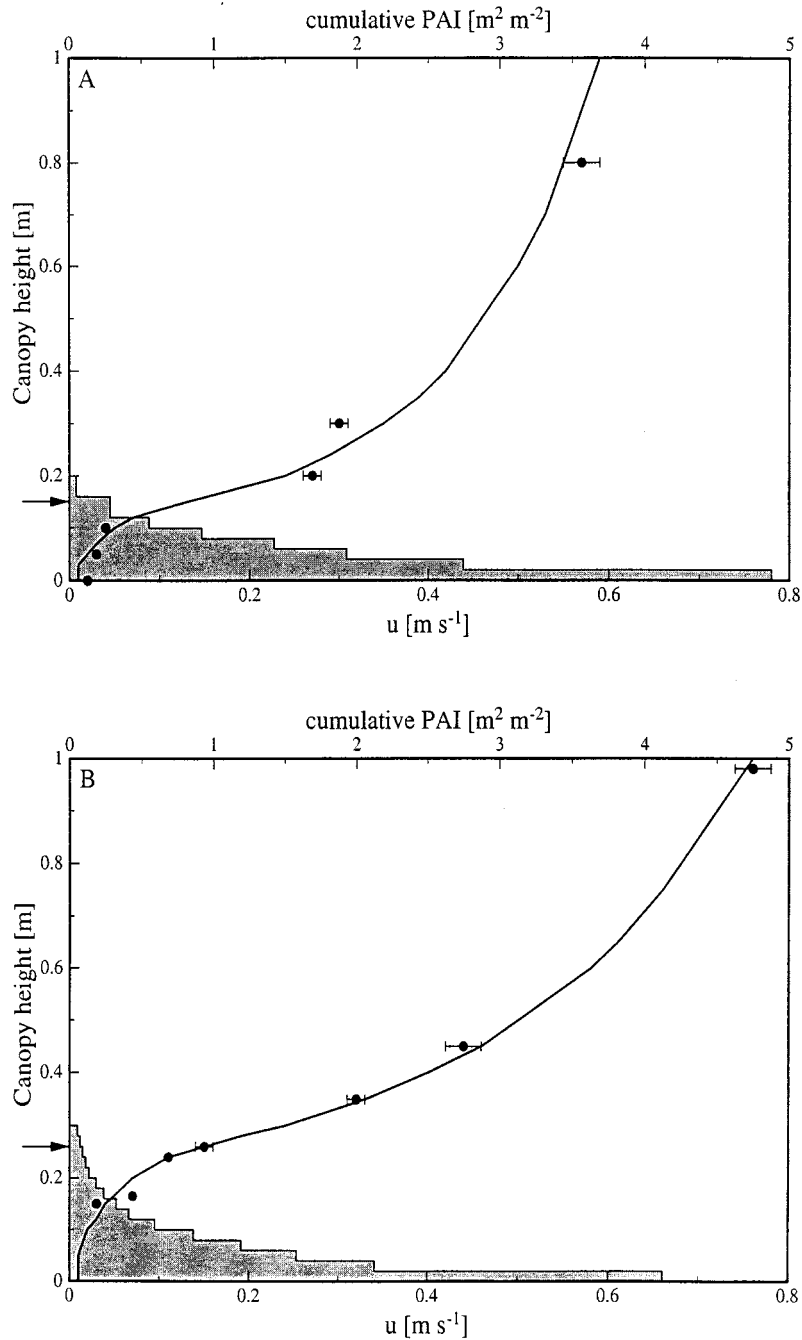
Fig. 2. Cumulative plant area index (PAI, hatched area), measured (symbols) and simulated (lines) profiles of wind speed above and within the canopies of the abandoned area (A), meadow (B) and pasture (C). Arrows indicate the upper height of the lower canopy layer formed mainly by forbs (error bars represent 1 standard error).
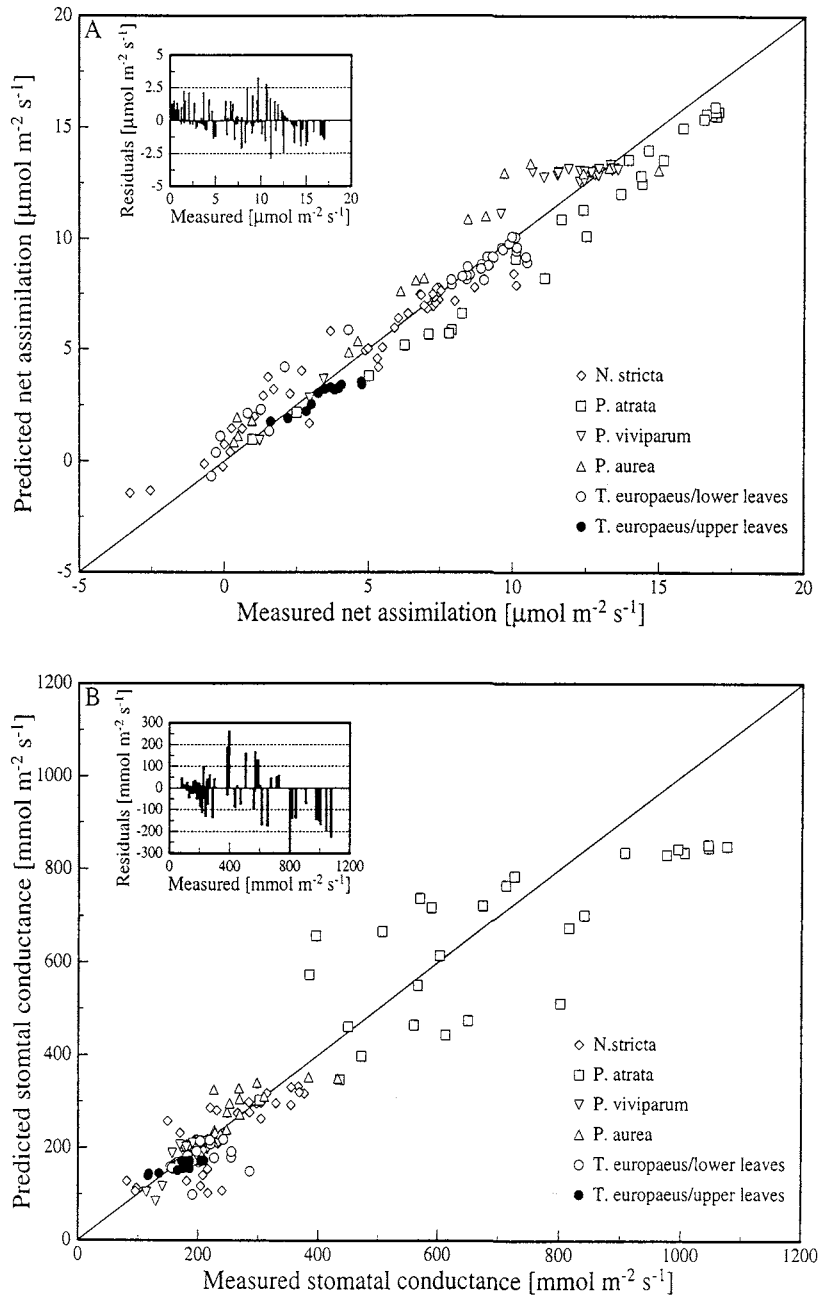
Fig. 3. Comparison between measured and predicted leaf net photosynthesis (A) and stomatal conductance (B) of the investigated species. Residuals (difference between predicted and measured values), for all species pooled, are shown as insets in the upper left corners.

Wang and Leuning, 1998) by introducing an empirical dependence of stomatal conductance on soil water availability into these models. Espe-

cially the parameter G_{fac}, which represents the sensitivity of stomata to the environmental factors considered in the model, to which stomatal con-

ductance is directly proportional (Eq. (10) of Wohlfahrt et al., 1998), should be adapted as the leaf water status becomes affected by alterations in soil water availability. This was indirectly accounted for in the present approach by parameterising the model of stomatal conductance separately for each site (Table 2B), thereby mapping the soil water availability of the site averaged over the growing season into the parameters of the stomatal conductance model (Wohlfahrt et al., 1998). The model, though, does not account for effects of diurnal and daily changes in plant water status on stomatal conductance. At the moment we consider this to be the source of the variation encountered in Fig. 3B and Table 5, which though remains to be verified by future investigations.

3.2.2. Leaf temperature

As shown in Fig. 4 correspondence between observed and predicted values of leaf temperature, including different species and sites, is fairly good, the correlation coefficients ranging between 0.69–0.99 (pooled 0.83, Table 5). For some species (e.g. *P. viviparum*, *N. stricta*) larger deviations from 1:1 correspondence occur, still the *F*-test is passed by each species, as well as by all species pooled (Table 5). The overall distribution of residuals around the predicted values may be regarded as symmetrical (Fig. 4), although leaf temperatures of some species (e.g. *N. stricta*) are slightly underestimated, whereas others (e.g. *P. viviparum*) tend to be overestimated. The underestimation of the leaf temperatures of *N. stricta* may be caused by the fact, that the leaves of this species are extremely narrow (approx. 0.3 mm leaf width). Since the leaves of *N. stricta* are grouped in bunches, which aerodynamically may behave as intact objects, similar to shoots of conifers (Nikolov et al., 1995), using the actual leaf width for calculating the leaf boundary layer conductance of *N. stricta* may underestimate the leaf boundary layer conductance and thus leaf temperature. Note that leaf widths have been taken as the characteristic dimension in the direction of the wind flow (Eqs. (1) and (2)). Thus for leaves whose length reaches several times their leaf width (*P. atrata*, *P. viviparum*, *N. stricta*), underestimation of the leaf boundary layer conductance may occur in the case of the wind flowing over the leaves perpendicular to their width.

Table 5

Results of a linear regression analysis of observed *versus* predicted values of net photosynthesis (A), stomatal conductance (g_{sv}), leaf temperature (T_l), wind speed (u), PPFD incident from above on a horizontal plane at different heights within the canopy ($PPFD_d(j)$), reflected short-wave ($Q_u(n)$), PPFD in the direct and diffuse components of the incoming short-wave radiation ($PPFD_{dif}(n+1)$ and $PPFD_{dir}(n+1)$) and incoming long-wave radiation ($L_o(n+1)$)[a]

Parameter	Site/Species	slope	y-intercept	r	F	$F_{crit.}$
A	Pooled	0.92 ± 0.02	0.64 ± 0.16	0.98	2695.80	6.81
G_{sv}	Pooled	0.85 ± 0.02	30.48 ± 9.05	0.95	1228.74	6.84
T_l	Pooled	0.76 ± 0.06	5.36 ± 1.35	0.83	154.07	7.01
u	A	1.02 ± 0.12	0.26 ± 0.10	0.91	73.94	8.68
	M	0.92 ± 0.07	0.22 ± 0.09	0.96	185.43	8.53
	P	1.07 ± 0.08	-0.08 ± 0.14	0.90	174.73	7.30
$PPFD_d(j)$	A	0.89 ± 0.02	57.50 ± 9.11	0.98	1309.80	7.08
	M	0.88 ± 0.01	73.60 ± 6.90	0.98	7822.89	6.70
	P	0.90 ± 0.01	23.67 ± 4.19	0.99	10 133.01	6.84
$Q_u(n)$	M	0.86 ± 0.01	2.94 ± 1.21	0.98	5498.55	6.76
$PPFD_{dif}(n+1)$	Pooled	1.04 ± 0.09	4.02 ± 20.62	0.80	123.03	7.00
$PPFD_{dir}(n+1)$	Pooled	0.89 ± 0.04	57.36 ± 46.88	0.92	403.98	7.00
$L_{o_d}(n+1)$	M	0.48 ± 0.02	171.03 ± 7.31	0.77	536.19	6.71

[a] Model performance is evaluated by the slope and the y-intercept of a regression line through observed *versus* predicted values (mean $\pm$ standard error), the Pearson's correlation coefficient (r) and by comparison of the F-value (F) with the critical F-value ($F_{crit.}$, F-value at $P = 0.01$) (A, abandoned area; M, meadow; P, pasture).
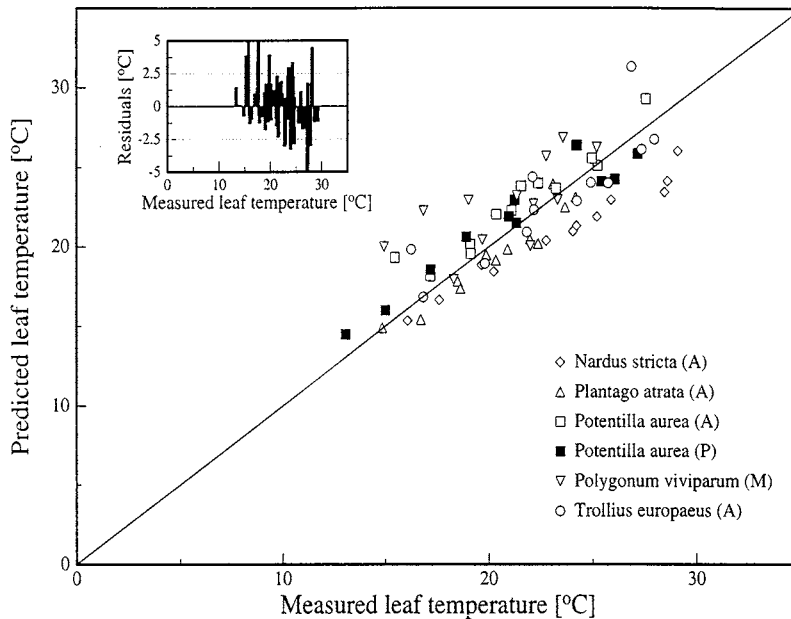
Fig. 4. Comparison between measured and predicted leaf temperatures of the investigated species. Residuals (difference between predicted and measured values), for all species/sites pooled, are shown as an inset in the upper left corner.

3.2.3. Wind profile

The correspondence between observed and predicted values of wind speed at the three sites is shown in Fig. 5. The distribution of the residuals around the predicted values may be regarded as symmetrical and the residuals do not exceed 0.5 m s^{-1}, except for a few exceptions. The correlation coefficients are higher than 0.90 and the y-intercepts as well as the slopes of linear regressions through the data in Fig. 5 are close to 0 and 1, respectively (Table 5). The model thus may be regarded to be well suited for describing the attenuation of wind speed within the investigated canopies.

3.2.4. Radiative transfer

The validity of the radiation profile predicted by the model of radiative transfer was assessed by two different approaches. Firstly, the PPFD measured by the means of ceptometers mounted horizontally at various heights within the canopy was compared with the predicted downward flux of PPFD incident on a horizontal plane at the same heights (Fig. 6A–C). Secondly, the reflected short-wave radiation (PPFD and NIR) measured above the canopy (data available only for the meadow) was compared with the predicted short-wave radiation leaving the uppermost canopy layer in the upward direction (Fig. 7).

The correspondence between observed and predicted values of the PPFD downward flux at various heights within the investigated canopies is shown in Fig. 6A–C. Altogether, the correlation coefficients and the F-values are high and the slopes and y-intercepts of the regressions lines are close to 1:1 correspondence (Table 5). A slight overestimation in the lower canopy layers is evident for the abandoned area and the meadow, an underestimation for the upper canopy layers of the meadow and pasture (Fig. 6A–C). In this context it should be noted, that minor deviations in height as a result of an uneven ground surface, either when positioning the ceptometers or during canopy structure analysis (Faurie et al., 1996), may have considerable effects on the resulting predictions, because a deviation in height of 1 cm may correspond to a difference in PAI of up to 1 m^2 m^{-2} in the lowest, very dense canopy layers.

The observed effects thus could represent artefacts arising from the experimental setup. The overestimation in the lower and the underestimation in the upper canopy layers may also be caused by the leaves not being distributed randomly, as assumed, but clumped in the lower and regular in the upper canopy layers. Markedly clumped leaf distributions for meadows and slightly clumped/regular leaf distributions for abandoned and differently stocked pastures have indeed been reported by Tappeiner and Cernusca (1989, 1998) for the Eastern Alps and the Central Caucasus. In these studies, leaf distribution was accounted for by empirically adjusting the leaf clustering factor so as to gain correspondence between measured (by the means of ceptometers) and predicted values of PPFD. It should be noted, that such an empirical adjustment is critical, because all the shortcomings of the model, as well as of the experimental approach are condensed into a single parameter, Ω (Tappeiner and Cernusca, 1989; Cescatti, 1997b). However, because statistical leaf distribution was not assessed in the present study,

we decided to maintain the assumption of a random leaf distribution. This is justified by the fact that our model, despite the small deviations mentioned above, generally predicts the penetration of PPFD well.

A less satisfying correspondence between measurements and predictions can be found for the reflected short-wave radiation, which is shown for the meadow in Fig. 7. As evident from the residuals, the model predicts low values of reflected short-wave radiation reasonably well, but increasingly underestimates higher values (see inset in Fig. 7 and slope and y-intercept in Table 5). This could result from scattering being underestimated in the NIR waveband, because minor deviations, as demonstrated above, were evident for the PPFD. Underestimation of scattering could occur because of the leaf scattering coefficient (Table 4) being too low in the NIR. The underestimation could also be attributed to simplifications implicit in Goudriaan's (1977) theory of radiative transfer (cf. Vygodskaya and Gorshokova, 1989). The Goudriaan model does not account for penumbra
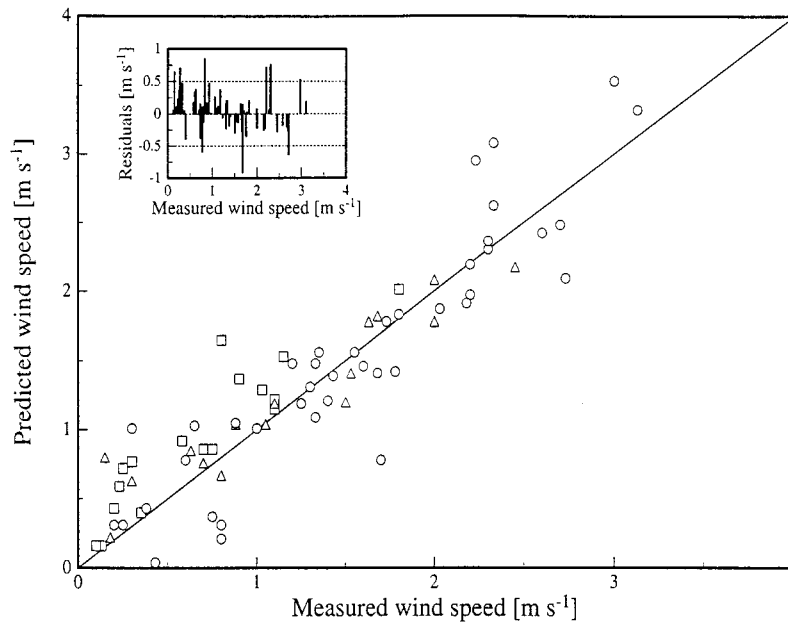

Fig. 5. Comparison between measured and predicted wind speeds at the abandoned area (squares), the meadow (triangles) and the pasture (circles). Residuals (difference between predicted and measured values), for all sites pooled, are shown as an inset in the upper left corner.
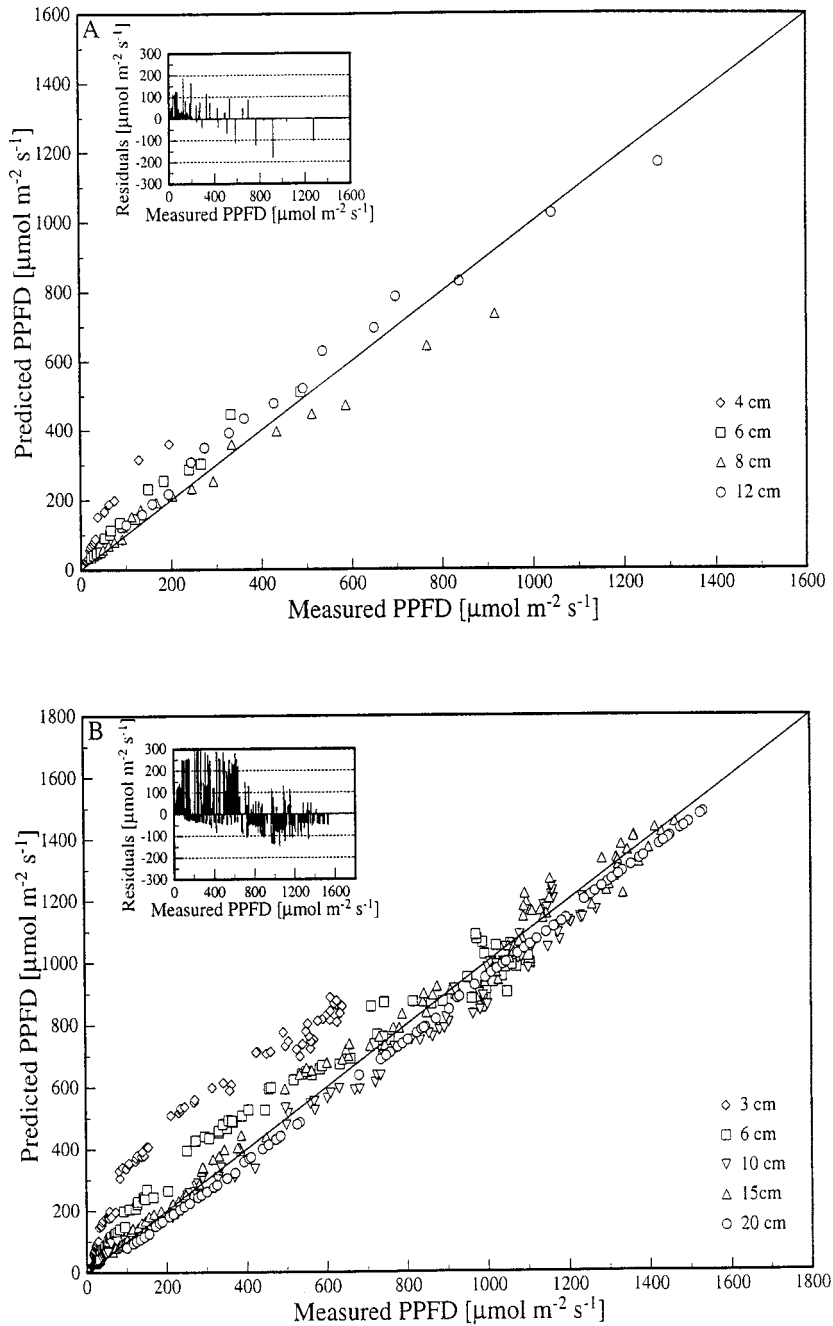
Fig. 6. Comparison between measured and predicted photosynthetic photon flux density (PPFD) incident from above on a horizontal plane at different heights within the canopies of the abandoned area (A), the meadow (B) and the pasture (C). Residuals (difference between predicted and measured values), for all heights pooled, are shown as insets in the upper left corners.
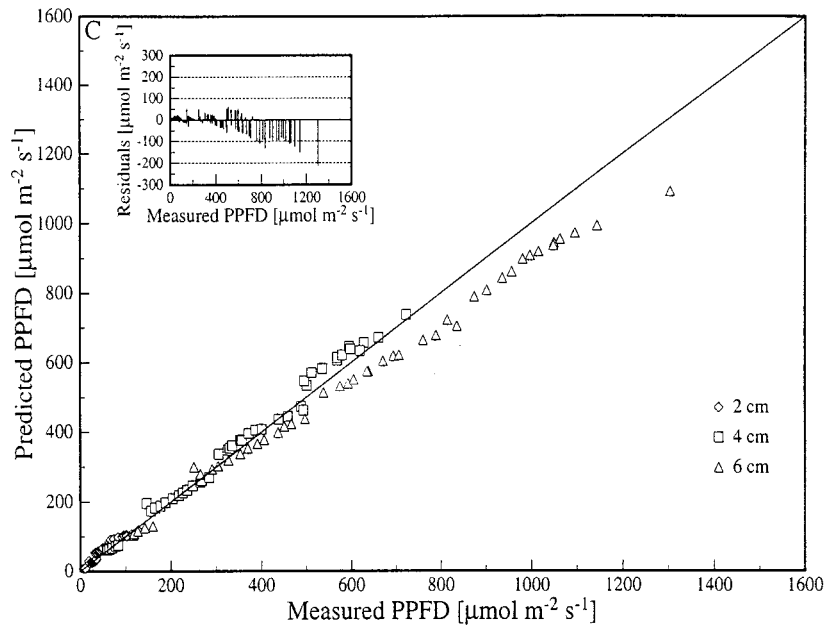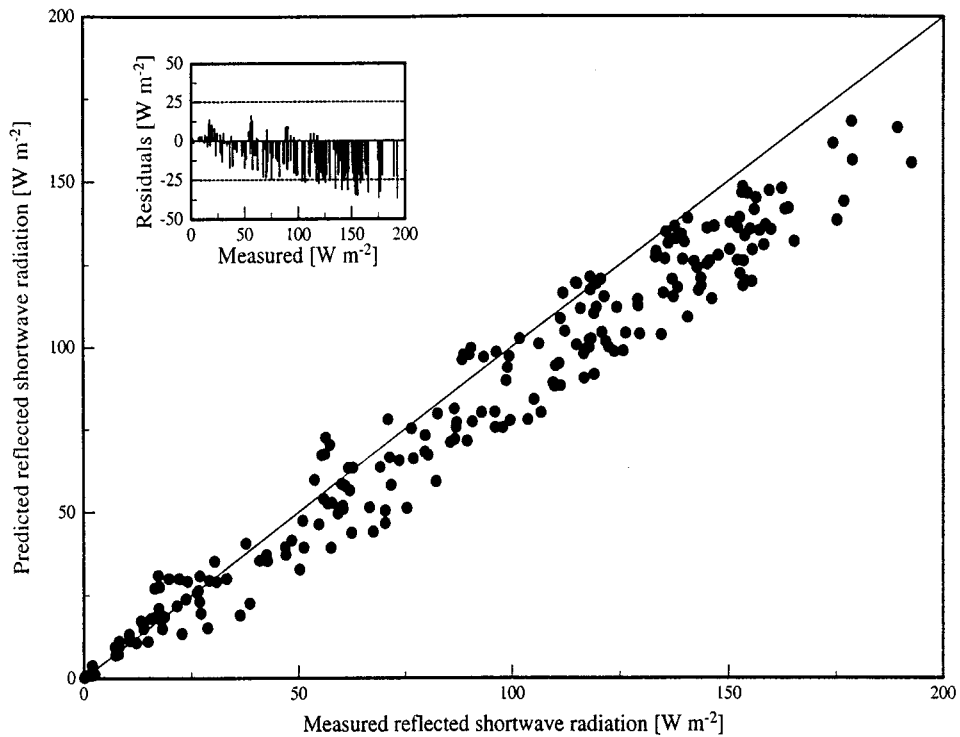
Fig. 6. (*Continued*)

Fig. 7. Comparison between measured and predicted reflected short-wave radiation above the meadow. Residuals (difference between predicted and measured values) are shown as an inset in the upper left corner.

(Stenberg, 1995) and infinite scattering of radiation, as approaches using transfer matrices do (Cescatti, 1997a; Royer et al., 1999). Moreover, reflected radiation is assumed to be distributed lambertian, not accounting for specular reflection (Asner and Wessman, 1997; Royer et al., 1999). Penumbra is significant only when the phytoelements are small and far apart from each other, as in coniferous forests (Stenberg, 1995), but not for grasslands, as in the present study. Multiple scattering and specular reflection of radiation are of minor importance for the PPFD (Asner and Wessman, 1997), where scattering is low anyhow (20%), but not in the NIR waveband, where scattering is high (80%). Yet, leaf temperatures are predicted reasonably well by the leaf energy balance, where the NIR absorbed by the leaves is an input parameter (Eq. (6)), underlining the validity of both the model of radiative transfer, as well as the leaf scattering coefficients. Moreover, preliminary results (Royer et al., in preparation) from a comparison to a model which accounts for infinite scattering and specular reflection of radiation

(Royer et al., 1999) suggest, that our model predicts scattering correctly, even in the NIR waveband.

3.2.5. Above canopy radiation

Irrespective of whether the direct and diffuse components of the incoming short-wave radiation have been measured or must be modelled (see Appendix B), the partitioning into the PPFD and NIR components has to be simulated at any rate (Fig. 1), because these entities have not been measured separately. The correspondence between observed and predicted values of PPFD in the direct and diffuse incoming short-wave radiation is shown in Fig. 8. The corresponding values have been calculated from measured values of the incoming total and diffuse short-wave radiation, from which the fraction of diffuse radiation (f_d) was inferred. The fraction of diffuse radiation, in turn, was used to derive atmospheric transmissivity (τ_a; Goudriaan and Van Laar, 1994), from which the fraction of PPFD was calculated according to Goudriaan (1977) (Table 6 in Ap-
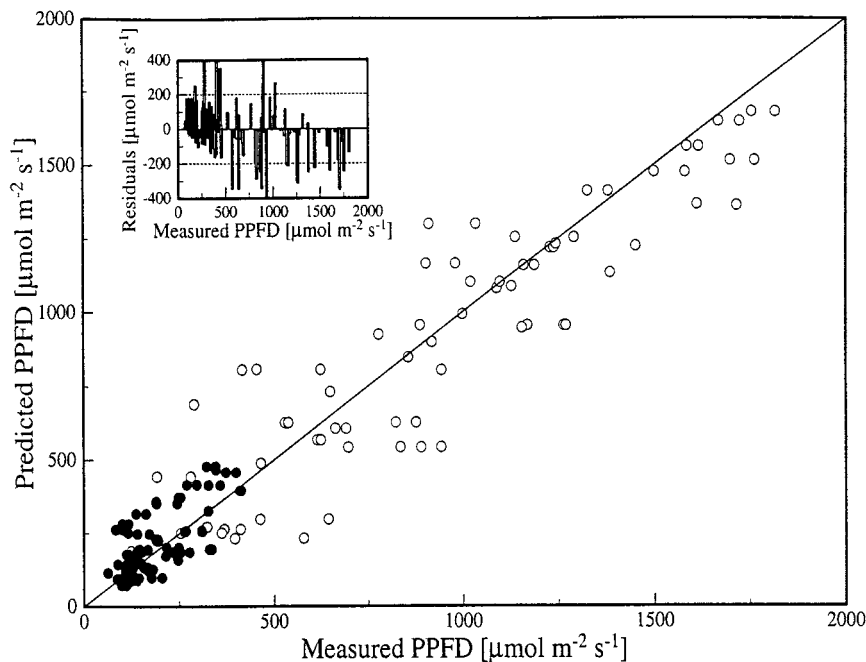

Fig. 8. Comparison between measured and predicted photosynthetic photon flux density (PPFD) in the incoming direct (open symbols) and diffuse (filled symbols) short-wave radiation. Residuals (difference between predicted and measured values) are shown as an inset in the upper left corner.

Table 6
Fraction of diffuse (f_d), photosynthetically active (f_{PPFD}) and near-infrared (f_{NIR}) radiation in the incoming short-wave radiation as a function of atmospheric transmissivity (τ_a)[a]

	$\tau_a < 0.3$	$0.3 \geq \tau_a \leq 0.7$	$\tau_a > 0.7$
f_d	1.0	$1.600 - 2.00 \cdot \tau_a$	0.2
f_{PPFD}	0.6	$0.675 - 0.25 \cdot \tau_a$	0.5
f_{NIR}	0.4	$0.325 - 0.25 \cdot \tau_a$	0.5

[a] According to Goudriaan (1977) and Goudriaan and Van Laar (1994).

pendix B). The slope and the y-intercept of the regression line for the diffuse PPFD data show closeness to 1:1 correspondence (Table 5), but the F-value and the correlation coefficient are somewhat lower than for the direct PPFD, indicating less quantitative correspondence, whereas a slight underestimation of the highest values leads to a comparably smaller qualitative correspondence for the direct PPFD (Fig. 8, Table 5).

Similar to short-wave radiation, the long-wave radiation incident from the sky may either be measured or modelled, as described in Appendix B. Fig. 9 shows the comparison between observed and predicted sky long-wave radiation. For the latter, cloud cover was arbitrarily fixed at an average value of 0.5, as a result of the lack of corresponding measurements. Given that the entire range of cloud cover situations (0–1) is equally represented in the measured data, using an average cloud cover of 0.5 should overestimate the lower and underestimate the higher long-wave fluxes, as it is indeed evident from Fig. 9, indicating that the model is capable to account for the variation in sky long-wave radiation with cloud cover.

4. Conclusion

A model is presented which aims at simulating the CO_2 and H_2O gas exchange of whole plants in their natural microenvironment, the canopy. For this purpose the model combines simulations at the leaf (gas exchange, energy balance) with simu-
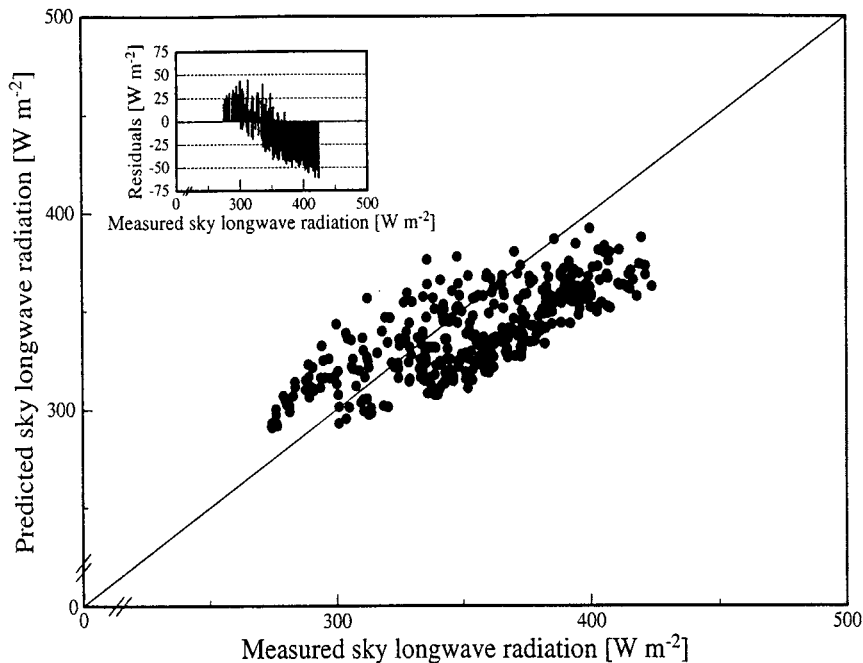

Fig. 9. Comparison between measured and predicted sky emitted long-wave radiation. Residuals (difference between predicted and measured values) are shown as an inset in the upper left corner.

lations at the canopy level (radiative transfer, wind attenuation). The model is parameterised for four forbs and one graminoid species occurring at three sites differing in land use, i.e. an abandoned area, a meadow and a pasture, using least squares fitting procedures to measured data. Each major submodel is validated separately against independently measured data, leading to generally satisfactory results. We thus feel that the model represents a suitable and useful tool for analysing the gas exchange of whole plants, and hence gain insights into the functioning of mountain grasslands. In the future the model will be applied to address some related questions, e.g. the role of plant architecture and leaf physiology in determining whole plant carbon gain.

Appendix A. The analytical solution to the leaf energy balance equation

An analytical solution to the leaf energy balance has been first proposed by Paw U (1987), in the present approach the form used by Nikolov et al. (1995) is adopted. If $e_s(T_l)$ in Eq. (6) is substituted for the polynomial from Eq. (12), the energy budget equation may be rearranged in the form of quartic equation for T_l, i.e.

$$T_l^4 + a_t \cdot T_l^3 + b_t T_l^2 + c_t \cdot T_l + d_t = 0, \tag{A1}$$

where the corresponding coefficients are given by

$$a_t = (8 \cdot \varepsilon_l \cdot \sigma \cdot 273.16 + 1.5842 \cdot 10^{-2} \cdot h_e) \cdot k_t, \tag{A2}$$

$$b_t = (12 \cdot \varepsilon_l \cdot \sigma \cdot 273.16^2 + 1.551861 \cdot h_e) \cdot k_t, \tag{A3}$$

$$c_t = (8 \cdot \varepsilon_l \cdot \sigma \cdot 273.16^3 + 44.513596 \cdot h_e + h_t) \cdot k_t \tag{A4}$$

and

$$d_t = (607.919 \cdot h_e - R_{abs} - h_t \cdot T_a - h_e \cdot e_a + 2 \cdot \varepsilon_l \cdot \sigma \cdot 273.16^4) \cdot k_t, \tag{A5}$$

in which

$$k_t = \frac{1}{2 \cdot \varepsilon_l \cdot \sigma + 5.82436 \cdot 10^{-4} \cdot h_e}, \tag{A6}$$

$$h_e = \frac{\rho \cdot c_p}{\gamma} g_{tv} \tag{A7}$$

and

$$h_l = 2 \cdot \rho \cdot c_p \cdot g_{bv} \cdot 0.924. \tag{A8}$$

Thereby it should be noted that conductances should have units of m s^{-1} in Eqs. (A7) and (A8). Since quartic equations may be solved analytically, it is possible to estimate leaf temperature without iteration for a given set of input variables (see Eq. (6)). Due to the inter-dependence of the leaf emitted long-wave flux on leaf temperature, there though still remains one iteration loop in the determination of leaf temperatures.

Appendix B. Solar geometry and above canopy radiation

The location of the sun in the sky is described in terms of its elevation above the horizon and its azimuth angle (Campbell and Norman, 1998). Assuming that leaves have no azimuthal preference, the position of the sun may be described solely by its elevation above the horizon (β) as

$$\sin \beta = \sin \phi \cdot \sin \delta + \cos \phi \cdot \cos \delta \cdot \cos[15 \cdot (t - t_0)], \tag{B1}$$

where ϕ is the latitude, δ the solar declination, t the local time and t_0 the time of solar noon. Solar

declination can be computed as

$$\sin \delta = 0.39785 \cdot \sin[278.97 + 0.9856 \cdot JD$$
$$+ 1.9165 \cdot \sin(356.6 + 0.9856 \cdot JD)], \quad (B2)$$

where JD stands for Julian Day ($JD = 1$ is January 1st). The time of solar noon is calculated from

$$t_0 = 12 - LC - ET, \quad (B3)$$

where ET is the equation of time and LC is the longitude correction, which is $\pm 1/15$ h for each degree east/west of the standard meridian. The equation of time depends on the day of the year and is calculated from

$$ET = (-104.7 \cdot \sin \varepsilon + 596.2 \cdot \sin 2 \cdot \varepsilon$$
$$+ 4.3 \cdot \sin 3 \cdot \varepsilon - 12.7 \cdot \sin 4 \cdot \varepsilon - 429.3 \cdot \cos \varepsilon$$
$$- 2.0 \cdot \cos 2 \cdot \varepsilon + 19.3 \cdot \cos 3 \cdot \varepsilon)/3600, \quad (B4)$$

where

$$\varepsilon = 279.575 + 0.9856 \cdot JD. \quad (B5)$$

The total solar radiation incident on a horizontal plane at the Earth's surface is given by

$$S_g = \tau_a \cdot S_c \cdot \sin \beta, \quad (B6)$$

where τ_a is the atmospheric transmissivity and S_c is the solar constant

$$S_c = 1367 \cdot \left(1 + 0.033 \cdot \cos\left[2 \cdot \pi \cdot \frac{(JD - 10)}{365}\right]\right), \quad (B7)$$

corrected for the eccentricity of the Earth's path around the sun (Goudriaan and Van Laar, 1994). The fraction of diffuse radiation is either calculated from measured values of total and diffuse (S_d) solar radiation as

$$f_d = \frac{S_d}{S_g}, \quad (B8)$$

or, if no measured values are available, calculated as a simple function of τ_a (Goudriaan and Van Laar, 1994), as depicted in Table 6, which then has to be specified a priori. The diffuse solar radiation is then given by

$$S_d = S_g \cdot f_d, \quad (B9)$$

and beam radiation is calculated as

$$S_b = S_g - S_d. \quad (B10)$$

The fractions of PPFD and NIR in the direct and diffuse components of solar radiation (f_{PPFD} and f_{NIR}, respectively) are calculated as simple functions of τ_a, as shown in Table 6 (Goudriaan, 1977). In the case that τ_a is not specified a priori, but f_d instead (because total and diffuse solar radiation have been measured), the relationships given for the calculation of f_d in Table 6 are used to inversely derive τ_a. The PPFD and NIR components of direct and diffuse solar radiation may then be calculated simply as the corresponding fraction times the direct and diffuse radiation flux, respectively.

The long-wave radiation originating from the sky either has to be measured, or, in the absence of measurements, it is calculated from air temperature and water vapour pressure at 2 m above ground and the fraction of the sky covered by clouds. The emissivity for long-wave radiation of a clear sky is given by (Brutsaert, 1984)

$$\varepsilon_{ac} = 1.72 \cdot \left(\frac{e_a}{10 \cdot T_{ak}}\right)^{1/7}. \quad (B11)$$

When clouds are present the emissivity is higher than for a clear sky, which may be accounted for using an equation given by Monteith and Unsworth (1990)

$$\varepsilon_a = (1 - 0.84 \cdot c) \cdot \varepsilon_{ac} + 0.84 \cdot c, \quad (B12)$$

where c is the fraction of the sky covered by clouds. The sky emitted long-wave radiation flux is then given by the well-known Stefan-Boltzmann equation

$$L_{o_d}(n + 1) = \varepsilon_a \cdot \sigma \cdot T_{ak}^4. \quad (B13)$$

Appendix C. Symbols and abbreviations

a	extinction coefficient for wind speed
A	net photosynthesis (μmol m^{-2} s^{-1})
a_t	coefficient in the analytical solution to the energy balance

B_l	normalised view factor		free convection (mmol m^{-2} s^{-1})
B_t	coefficient in the analytical solution to the energy balance	g_{bvf}	single-sided leaf boundary layer conductance to water vapour, if heat exchange is dominated by forced convection (mmol m^{-2} s^{-1})
B_u	weights according to the Uniform Overcast Sky		
C	factor indicating sky cloud cover		
C_a	CO_2 partial pressure in the ambient air (Pa)	G_{fac}	stomatal sensitivity coefficient
c_{fm}	factor converting conductances from units of mmol m^{-2} s^{-1} to m s^{-1}	g_{min}	minimum stomatal conductance to water vapour (mmol m^{-2} s^{-1})
		g_{sv}	stomatal conductance to water vapour (mmol m^{-2} s^{-1})
C_i	Internal CO_2 partial pressure (Pa)	g_{tv}	leaf total conductance to water vapour (mmol m^{-2} s^{-1})
C_N	slope of linear relationship relating N_L to V_{cmax} (µmol CO_2 mmol N^{-1} s^{-1})	h	upper height of the lower canopy layer formed mainly by forbs (m)
c_p	specific heat of dry air (1010 J kg^{-1} K^{-1})	H	sensible heat loss (W m^{-2})
C_s	leaf surface CO_2 partial pressure (Pa)	h_e	auxiliary variable in the analytical solution to the energy balance
		h_s	leaf surface relative humidity
c_t	Coefficient in the analytical solution to the energy balance	h_t	auxiliary variable in the analytical solution to the energy balance
C_0	y-intercept of linear relationship relating N_L to V_{cmax} (µmol CO_2 m^{-2} s^{-1})	I_{fac}	coefficient representing the extent to which R_{dark} is inhibited in the light
d	zero plane displacement (m)	j	subscript indicating canopy layer
d_t	coefficient in the analytical solution to the energy balance	JD	Julian Day
E_a	air water vapour pressure (hPa)	k_t	auxiliary variable in the analytical solution to the energy balance
$e_s(T_l)$	saturated leaf water vapour pressure (hPa)	L	latent heat of vaporisation (J K^{-1})
ET	equation of time (decimal)	LC	longitude correction (decimal)
F	fraction of leaves in leaf angle class	L_0	long-wave radiation incident on leaves (W m^{-2})
f_d	fraction of diffuse radiation in total short-wave radiation	L_{o_d}	downward flux of long-wave radiation (W m^{-2})
f_{NIR}	fraction of NIR in direct and diffuse short-wave radiation, respectively	L_{o_e}	leaf emitted long-wave radiation (W m^{-2})
f_{PPFD}	fraction of PPFD in direct and diffuse short-wave radiation, respectively	L_{o_u}	upward flux of long-wave radiation (W m^{-2})
		NIR	near infrared radiation (W m^{-2})
f_{sl}	fraction of sunlit leaves	M_i	probability of interception
g_{bv}	single-sided leaf boundary layer conductance to water vapour (mmol m^{-2} s^{-1})	M_t	probability of non-interception
		$O(\beta, \lambda)$	projection of leaves with inclination λ into inclination β
g_{bve}	single-sided leaf boundary layer conductance to water vapour, if heat exchange is dominated by	$O(\beta', \lambda)$	Projection of leaves with inclination λ into inclination β'
		P	Air pressure (hPa)

p	Subscript indicating whole plant layer		T_a	air temperature (°C)
PAI	Total plant area index (m^2 m^{-2})		T_{ak}	air temperature (K)
P_{fac}	Ratio between P_{ml} and V_{cmax} at the reference temperature of 293.16 K		T_l	leaf temperature (°C)
			T_{lk}	leaf temperature (K)
			T_{lksl}	leaf temperature of sunlit leaves (K)
P_{ml}	Potential rate of RuBP regeneration (μmol m^{-2} s^{-1})		T_{lksh}	leaf temperature of shaded leaves (K)
PPFD	photosynthetic photon flux density (μmol m^{-2} s^{-1})		T_{sk}	soil temperature (K)
Q_d	downward flux of total short-wave radiation (W m^{-2})		t_0	time of solar noon (decimal)
			U	wind speed (m s^{-1})
			$u*$	friction velocity (m s^{-1})
Q_{dir}	downward flux of beam radiation (W m^{-2})		V_{cmax}	maximum rate of carboxylation (μmol m^{-2} s^{-1})
Q_i	intercepted total short-wave radiation (W m^{-2})		$V_{cmax}(T_{ref})$	maximum rate of carboxylation at the reference temperature of 293.16 K in the absence of any deactivation as a result of high temperature (μmol m^{-2} s^{-1})
Q_{shade}	short-wave radiation incident on shaded leaves (W m^{-2})			
Q_{sun}	short-wave radiation incident on sunlit leaves (W m^{-2})		W	leaf width (m)
			z	canopy height (m)
Q_u	upward flux of total short-wave radiation (W m^{-2})		z_0	momentum roughness parameter (m)
R_{abs}	bi-directional absorbed short-wave and long-wave radiation (W m^{-2})		*Greek*	
			α	apparent quantum yield of net photosynthesis at saturating CO_2 (mol CO_2 mol photons^{-1})
R_{dark}	dark respiration rate (μmol m^{-2} s^{-1})		β	elevation of sun (radians)
			β'	elevation of nine sky angle classes (radians)
R_{fac}	ratio between R_{dark} and V_{cmax} at the reference temperature of 293.16 K		χ_1	avelength dependent leaf scattering coefficient
			χ_s	wavelength dependent soil scattering coefficient
RUBISCO	Ribulose-1,5-bisphosphate carboxylase/oxygenase		δ	latitude (radians)
RuBP	Ribulose-1,5-bisphosphate		ΔH_a	energy of activation (J mol^{-1})
S_b	direct solar radiation incident on a horizontal plane above the canopy (W m^{-2})		ΔH_d	energy of deactivation (J mol^{-1})
			ΔL	plant area index in canopy layer (m^2 m^{-2})
S_c	solar constant (W m^{-2})		ΔS	entropy term (J K^{-1} mol^{-1}) coefficient in calculation of *ET*
S_d	diffuse solar radiation incident on a horizontal plane above the canopy (W m^{-2})			
S_g	total solar radiation incident on a horizontal plane above the canopy (W m^{-2})		ε_a	sky thermal emissivity as a function of cloud cover
t	local time (decimal)		ε_{ac}	clear sky thermal emissivity

ε_l	leaf thermal emissivity (0.96)
ε_s	soil thermal emissivity (0.96)
ϕ	solar declination (radians)
γ	psychrometric constant (Pa K^{-1})
λ	leaf angle (radians)
λE	latent heat loss (W m^{-2})
ρ	density of dry air (kg m^{-3})
σ	Stefan-Boltzmann constant ($5.6697 \cdot 10^{-8}$ W m^{-2} K^{-4})
τ_a	atmospheric transmissivity
Ω	leaf clustering factor

References

Aalto, T., Vesala, T., Mattila, T., Simbierowicz, P., Hari, P., 1999. A three-dimensional stomatal CO_2 exchange model including gaseous phase and leaf mesophyll separated by irregular interface. J. Theor. Biol. 196, 115–128.

Aber, J.D., 1997. Why don't we believe the models. Bull. Ecol. Soc. Am. 78, 232–233.

Amthor, J.S., 1994. Scaling CO_2-photosynthesis relationships from the leaf to the canopy. Photosynth. Res. 39, 321–350.

Anten, N.P.R., Werger, M.J.A., 1996. Canopy structure and nitrogen distribution in dominant and subordinate plants in a dense stand of *Amarathus dubius* L. with a size hierarchy of individuals. Oecologia 105, 30–37.

Anten, N.P.R., Hernandez, R., Medina, E.M., 1996. The photosynthetic capacity and nitrogen concentration as related to light regime in shade leaves of a montane tropical forest tree, *Tetrorchidium rubrivenium*. Funct. Ecol. 10, 491–500.

Asner, G.P., Wessman, C.A., 1997. Scaling PAR absorption from the leaf to the landscape level in spatially heterogeneous ecosystems. Ecol. Model. 103, 81–97.

Badger, M.R., Collatz, G.J., 1977. Studies on the kinetic mechanism of ribulose-1,5-bisphosphate carboxylase and oxygenase reactions, with particular reference to the effect of temperature on kinetic parameters. Year Book Carnegie Inst. Washington 76, 355–361.

Bahn, M., Cernusca, A., 1999. Effects of land-use changes on plants-a functional approach relating plant and ecosystem processes. In: Cernusca, A., Tappeiner, U., Bayfield, N. (Eds.), Land-use Changes in European Mountain Ecosystems. ECOMONT — Concepts and Results, Blackwell Wissenschafts-Verlag, Berlin, pp. 150–160.

Bahn, M., Cernusca, A., Tappeiner, U., Tasser, E., 1994. Wachstum krautiger Arten auf einer Mähwiese und einer Almbrache. Ver. Ges. Ökol. 23, 23–30.

Baldocchi, D.D., 1992. A Lagrangian random walk model for simulating water vapor, CO_2 and sensible heat flux densities and scalar profiles over and within a soybean canopy. Boundary Layer Meteorol. 61, 113–144.

Baldocchi, D.D., 1993. Scaling water vapor and carbon dioxide exchange from leaves to canopy: rules and tools. In: Ehleringer, J.R., Field, C.B. (Eds.), Scaling Physiological Processes: Leaf to Globe. Academic Press, San Diego, pp. 77–116.

Baldocchi, D.D., 1997. Measuring and modelling carbon dioxide and water vapor exchange over a temperate broad-leaved forest during the 1995 summer drought. Plant Cell Environ. 20, 1108–1122.

Baldocchi, D.D., Collineau, S., 1994. The physical nature of solar radiation in heterogeneous canopies: Spatial and temporal attributes. In: Caldwell, M.M., Pearcy, R.W. (Eds.), Exploitation of Environmental Heterogeneity by Plants. Academic Press, San Diego, pp. 21–71.

Baldocchi, D.D., Harley, P.C., 1995. Scaling carbon dioxide and water vapor exchange from leaf to canopy in a deciduous forest. II. Model testing and application. Plant Cell Environ. 18, 1157–1173.

Baldocchi, D.D., Meyers, T., 1998. On using eco-physiological, micrometeorological and biogeochemical theory to evaluate carbon dioxide, water vapor and trace gas fluxes over vegetation: a perspective. Agric. For. Meteorol. 90, 1–25.

Ball, J.T., Woodrow, I.E., Berry, J.A., 1987. A model predicting stomatal conductance and its contribution to the control of photosynthesis under different environmental conditions. In: Biggens, J. (Ed.), Progress in Photosynthesis Research Vol. IV, Proceedings of the VII International Congress on Photosynthesis. Martinus Nijhoff, Dordrecht, pp. 221–224.

Barnes, P.W., Beyschlag, W., Ryel, R., Flint, S.D., Caldwell, M.M., 1990. Plant competition for light analyzed with a multispecies canopy model III. Influence of canopy structure in mixtures and monocultures of wheat and wild oat. Oecologia 82, 560–566.

Berry, J.A, Collatz, G.J., Denning, A.S., Colello, G.D., Fu, W., Grivet, C., et al., 1998. SiB2, a model for simulation of biological processes within a climate model. In: Van Gardingen, P.R., Foody, G.M., Curran, P.J. (Eds.), Scaling-up: From Cell to Landscape, Society of Experimental Biology Seminar Series 63. Cambridge University Press, Cambridge, pp. 347–369.

Beyschlag, W., Barnes, P.W., Ryel, R., Caldwell, M.M., Flint, S.D., 1990. Plant competition for light analyzed with a multispecies canopy model II. Influence of photosynthetic characteristics on mixtures of wheat and wild oat. Oecologia 82, 374–380.

Boegh, E., Soegaard, H., Friborg, T., Levy, P.E., 1999. Models of CO_2 and water vapour fluxes from a sparse millet crop in the Sahel. Agric. For. Meteorol. 93, 7–26.

Brutsaert, W., 1984. Evaporation into the Atmosphere: Theory, History, and Applications. D. Reidel, Boston, p. 299.

Buck, A.L., 1981. New equations for computing vapor pressure and enhancement factor. J. Appl. Meteorol. 20, 1527–1532.

Caldwell, M.M., Meister, H.-P., Tenhunen, J.D., Lange, O.L., 1986. Canopy structure, light microclimate and leaf gas exchange of *Quercus coccifera* L. in a Portuguese

macchia: measurements in different canopy layers and simulations with a canopy model. Trees 1, 25–41.

Campbell, G.S., Norman, J.M., 1998. An Introduction to Environmental Biophysics, 2nd Edition. Springer, New York, p. 286.

Cernusca, A., 1977. Bestandesstruktur, Mikroklima, Bestandesklima und Energiehaushalt von Pflanzenbeständen des alpinen Grasheidegürtels in den Hohen Tauern. Erste Ergebnisse der Projekstudie 1976. In: Cernusca, A. (Ed.), Alpine Grasheide Hohe Tauern. Ergebnisse der Ökosystemstudie 1976, Veröffentlichungen des Österreichischen MaB-Hochgebirgsprogrammes Hohe Tauern Band 1. Universitätsverlag Wagner, Innsbruck, pp. 25–45.

Cernusca, A., 1987. Application of computer methods in the field to assess ecosystem function and response to stress. In: Tenhunen, J.D., Catarino, F.M., Lange, O.L., Oechel, W.C. (Eds.), Plant Response to Stress, NATO ASI Series, vol. G15. Springer, Berlin, pp. 157–164.

Cernusca, A., Seeber, M.C., 1981. Canopy structure, microclimate and the energy budget in different alpine plant communities. In: Grace, J., Ford, E.D., Jarvis, P.G. (Eds.), Plants and their Atmospheric Environment, 21st Symposium of The British Ecological Society. Blackwell, Oxford, pp. 75–81.

Cernusca, A., Bahn, M., Chemini, C., Graber, W., Siegwolf, R., Tappeiner, U., et al., 1998. ECOMONT: a combined approach of field measurements and process-based modelling for assessing effects of land-use changes in mountain landscapes. Ecol. Model. 113, 167–178.

Cescatti, A., 1997a. Modelling the radiative transfer in discontinuous canopies of asymmetric crowns. I. Model structure and algorithms. Ecol. Model. 101, 263–274.

Cescatti, A., 1997b. Modelling the radiative transfer in discontinuous canopies of asymmetric crowns. II. Model testing and application in a Norway spruce stand. Ecol. Model. 101, 275–284.

Cescatti, A., Chemini, C., De Siena, C., Gianelle, D., Nicolini, G., Wohlfahrt, G., 1999. Monte Bondone composite landscape, Italy. In: Cernusca, A., Tappeiner, U., Bayfield, N. (Eds.), Land-use Changes in European Mountain Ecosystems. ECOMONT — Concepts and Results, Blackwell Wissenschafts-Verlag, Berlin, pp. 60–73.

Chen, J.-L., Reynolds, J.F., Harley, P.C., Tenhunen, J.D., 1993. Coordination theory of leaf nitrogen distribution in a canopy. Oecologia 93, 63–69.

Cionco, R.M., 1972. A wind profile index for canopy flow. Boundary Layer Meteorol. 3, 255–263.

De Pury, D.G.G., Farquhar, G.D., 1997. Simple scaling of photosynthesis from leaves to canopies without the errors of big-leaf models. Plant Cell Environ. 20, 537–557.

De Wit, C.T., 1965. Photosynthesis of Leaf Canopies. Agricultural Research Report No. 663, Pudoc, Wageningen, 57 pp.

Falge, E., 1997. Die Modellierung der Kronendachtranspiration von Fichtenbeständen (Picea *abies* (L.) Karst.). PhD thesis, Bayreuther Forum Ökologie Band 48, Universität Bayreuth, Bayreuth, 221 pp.

Falge, E., Graber, W., Siegwolf, R., Tenhunen, J.D., 1996. A model of the gas exchange of *Picea abies* to habitat conditions. Trees 10, 277–287.

Farquhar, G.D., Sharkey, T.D., 1982. Stomatal conductance and photosynthesis. Ann. Rev. Plant Physiol. 33, 317–342.

Faurie, O., Soussana, J.F., Sinoquet, H., 1996. Radiation interception, partitioning and use in grass-clover mixtures. Ann. Bot. 77, 35–45.

Field, C.B., 1983. Ecological scaling of carbon gain to stress and resource availability. In: Mooney, H.A., Winner, W.E., Pell, E.J. (Eds.), Response of Plants to Multiple Stresses, Physiological Ecology: a Series of Monographs, Texts and Treatises. Academic Press, San Diego, pp. 35–65.

Friend, A.D., 1995. PGEN: an integrated model of leaf photosynthesis, transpiration and conductance. Ecol. Model. 77, 233–255.

Gandolfo, C., Sulli, M., 1993. Studi sul clima del Trentino per ricerche dendroclimatologiche e di ecologia forestale, Provincia Autonoma di Trento-Servizio Foreste, Caccia e Pesca, 83 pp.

Goudriaan, J., 1977. Crop micrometeorology: a simulation study. Simulation Monographs, Centre for Agricultural Publishing and Documentation, Pudoc, Wageningen, 248 pp.

Goudriaan, J., 1988. The bare bones of leaf angle distribution in radiation models for canopy photosynthesis and energy exchange. Agric. For. Meteorol. 43, 155–169.

Goudriaan, J., Van Laar, H.H., 1994. Modelling Crop Growth Processes. Kluwer, Amsterdam, p. 238.

Harley, P.C., Thomas, R.B., Reynolds, J.F., Strain, B.R., 1992. Modelling photosynthesis of cotton grown under elevated CO_2. Plant Cell Environ. 15, 271–282.

Hikosaka, K., Hirose, T., 1998. Leaf and canopy photosynthesis of C_3 plants at elevated CO_2 in relation to optimal partitioning of nitrogen among photosynthetic components: theoretical prediction. Ecol. Model. 106, 247–259.

Hikosaka, K., Terashima, I., 1995. Comparative ecophysiology of leaf and canopy photosynthesis. Plant Cell Environ. 18, 1111–1128.

Hikosaka, K., Terashima, I., 1996. Nitrogen partitioning among photosynthetic components and its consequences in sun and shade plants. Funct. Ecol. 10, 335–343.

Hirose, T., Werger, M.J.A., 1987a. Nitrogen use efficiency in instantaneous and daily photosynthesis of leaves in the canopy of a *Solidago altissima* stand. Physiol. Plant. 70, 215–222.

Hirose, T., Werger, M.J.A., 1987b. Maximizing daily canopy photosynthesis with respect to the leaf nitrogen allocation pattern in the canopy. Oecologia 72, 520–526.

Huntingford, C., Cox, P.M., 1997. Use of statistical and neural network techniques to detect how stomatal conductance responds to changes in the local environment. Ecol. Model. 97, 217–246.

Jarvis, P.G., 1976. The interpretation of the variations in leaf water potential and stomatal conductance found in canopies in the field. Philos. Trans. Roy. Soc. Lond. Ser. B 273, 593–610.

Jarvis, P.G., McNaughton, K.G., 1986. Stomatal control of transpiration: scaling up from leaf to region. Adv. Ecol. Res. 15, 1–48.

Jones, H.G., 1998. Stomatal control of photosynthesis and transpiration. J. Exp. Bot. 49, 387–398.

Jordan, D.B., Ogren, W.L., 1984. The CO_2/O_2 specificity of ribulose-1,5-bisphosphate carboxylase/oxygenase. Dependence on ribulose-bisphosphate concentration, pH and temperature. Planta 161, 308–313.

Kirschbaum, M.U.F., Gross, L.J., Pearcy, R.W., 1988. Observed and modelled stomatal responses to dynamic light environments in the shade plant *Alocasia macrorrhiza*. Plant Cell Environ. 11, 111–121.

Körner, Ch., Scheel, J.A., Bauer, H., 1979. Maximum leaf diffusive conductance in vascular plants. Photosynthetica 13, 45–82.

Kull, O., Jarvis, P.G., 1995. The role of nitrogen in a simple scheme to scale up photosynthesis from leaf to canopy. Plant Cell Environ. 18, 1174–1182.

Leuning, R., 1995. A critical appraisal of a combined stomatal-photosynthesis model for C_3 plants. Plant Cell Environ. 18, 339–355.

Leuning, R., Kelliher, F.M., De Pury, D.G.G., Schulze, E.D., 1995. Leaf nitrogen, photosynthesis, conductance and transpiration: scaling from leaves to canopies. Plant Cell Environ. 18, 1183–1200.

Lloyd, J., Grace, J., Miranda, A.C., Meir, P., Wong, S.C., Miranda, H.C., et al., 1995. A simple calibrated model of Amazon rainforest productivity based on leaf biochemical properties. Plant Cell Environ. 18, 1129–1145.

Maki, T., 1975. Interrelationships between zero-plane displacement, aerodynamic roughness length and plant canopy height. J. Agric. Meteorol. 31, 61–70 Japanese text, English summary and figure lengths.

Monsi, M., Saeki, T., 1953. Über den Lichtfaktor in den Pflanzengesellschaften und seine Bedeutung für die Stoffproduktion. Jap. J. Bot. 14, 22–52.

Monteith, J.L., Unsworth, M.H., 1990. Principles of Environmental Physics, 2nd Edition. Edward Arnold, London, p. 291.

Nikolov, N.T., Massman, W.J., Schoettle, A.W., 1995. Coupling biochemical and biophysical processes at the leaf level: an equilibrium photosynthesis model for leaves of C_3 plants. Ecol. Model. 80, 205–235.

Nilson, T., 1971. A theoretical analyses of the frequency of gaps in plant stands. Agric. Meteorol. 8, 25–38.

Nobel, P.S., 1991. Physicochemical and Environmental Plant Physiology. Academic Press, San Diego, p. 635.

Norman, J.M., 1993. Scaling processes between leaf and canopy levels. In: Ehleringer, J.R., Field, C.B. (Eds.), Scaling Physiological Processes: Leaf to Globe. Academic Press, San Diego, pp. 41–76.

Oke, T.R., 1987. Boundary Layer Climates, 2nd Edition. Routledge, London, p. 435.

Pachepsky, L.B., Haskett, J.D., Acock, B., 1996. An adequate model of photosynthesis I. Parameterization, validation and comparison of models. Agric. Systems 50, 209–225.

Pachepsky, L.B., Acock, B., 1996. A model 2DLEAF of leaf gas exchange: development, validation and ecological application. Ecol. Model. 93, 1–18.

Paw U, K.T., 1987. Mathematical analysis of the operative temperature and energy budget. J. Therm. Biol. 12, 227–233.

Pereira, A.R., Shaw, R.H., 1980. A numerical experiment on the mean wind structure inside canopies of vegetation. Agric. Meteorol. 22, 303–318.

Ross, J., 1975. Radiative transfer in plant communities. In: Monteith, J.W. (Ed.), Vegetation and the Atmosphere. Academic Press, London, pp. 13–55.

Ross, J., 1981. The Radiation Regime and Architecture of Plant Stands. Junk Publisher, The Hague, p. 391.

Royer, S., Cernusca, A., Tappeiner, U., Royer, A., 1999. A model for multi-species grassland canopies. In: Cernusca, A., Tappeiner, U., Bayfield, N. (Eds.), Land-use Changes in European Mountain Ecosystems. ECOMONT — Concepts and Results, Blackwell Wissenschafts-Verlag, Berlin, pp. 194–198.

Sala, A., Tenhunen, J.D., 1996. Simulations of canopy net photosynthesis and transpiration in *Quercus ilex* L. under the influence of seasonal drought. Agric. For. Meteorol. 78, 203–222.

Schulze, E.-D., Chapin, F.S4 . III, 1987. Plant specialisation to environments of different resource availability. In: Schulze, E.-D., Zwölfer, H. (Eds.), Potentials and Limitations to Ecosystem Analysis, Ecological Studies 61. Springer, Berlin, pp. 120–147.

Sellers, P.J., Berry, J.A., Collatz, G.J., Field, C.B., Hall, F.G., 1992. Canopy reflectance, photosynthesis, and transcription. III. A reanalysis using improved leaf models and a new canopy integration scheme. Remote Sens. Environ. 42, 187–216.

Spitters, C.J.T., 1986. Separating the diffuse and direct component of global radiation and its implication for modelling canopy photosynthesis. Part II. Calculation of canopy photosynthesis. Agric. For. Meteorol. 38, 231–242.

Stenberg, P., 1995. Penumbra in within-shoot and between-shoot shading in conifers and its significance for photosynthesis. Ecol. Model. 77, 215–231.

Su, H.-B., Paw U, K.T., Shaw, R.H., 1996. Development of a coupled leaf and canopy model for the simulation of plant-atmosphere interaction. J. Appl. Meteorol. 35, 733–748.

Tappeiner, U., Cernusca, A., 1989. Canopy structure and light climate of different Alpine plant communities: analysis by means of a model. Theor. Appl. Climatol. 40, 81–92.

Tappeiner, U., Cernusca, A., 1991. The combination of measurements and mathematical modelling for assessing canopy structure effects. In: Esser, G., Overdieck, D. (Eds.), Facets of Modern Ecology: Basic and Applied Aspects. Elsevier, Amsterdam, pp. 161–193.

Tappeiner, U., Cernusca, A., 1994. Bestandesstruktur, Energiehaushalt und Bodenatmung einer Mähwiese, einer Almweide und einer Almbrache. Ver. Ges. Ökol. 23, 49–56.

Tappeiner, U., Cernusca, A., 1998. Model simulation of spatial distribution of photosynthesis in structurally differing plant communities in the Central Caucasus. Ecol. Model. 113, 201–223.

Tappeiner, U., Sapinsky, S., 1999. Canopy structure, primary production and litter decomposition. In: Cernusca, A., Tappeiner, U., Bayfield, N. (Eds.), Land-use Changes in European Mountain Ecosystems. ECOMONT — Concepts and Results, Blackwell Wissenschafts-Verlag, Berlin, pp. 127–129.

Tardieu, F., Simmoneau, T., 1998. Variability among species of stomatal control under fluctuating soil water status and evaporative demand, modelling isohydric and anisohydric behaviour. J. Exp. Bot. 49, 419–432.

Tasser, E., Prock, S., Mulser, J., 1999. Impact of land use on vegetation along the Eastern Alpine transect. In: Cernusca, A., Tappeiner, U., Bayfield, N. (Eds.), Land-use Changes in European Mountain Ecosystems. ECOMONT — Concepts and Results, Blackwell Wissenschafts-Verlag, Berlin, pp. 235–246.

Tenhunen, J.D., 1999. Model hierarchies for relating vegetation structure, ecosystem physiology, and plant community distribution to landscape water use. In: Cernusca, A., Tappeiner, U., Bayfield, N. (Eds.), Land-use Changes in European Mountain Ecosystems. ECOMONT — Concepts and Results, Blackwell Wissenschafts-Verlag, Berlin, pp. 199–204.

Verstraete, M.M., 1985. A soil-vegetation-atmosphere model for micrometeorological research in arid regions. Cooperative Thesis No. 88, Massachusetts Institute of Technology and National Center for Atmospheric Research, Boulder.

Vesala, T., Ahonen, T., Hari, P., Krissinel, E., Shokhirev, N., 1996. Analysis of stomatal CO_2 uptake by a three-dimensional cylindrically symmetric model. New Phytol. 132, 235–245.

Von Caemmerer, S., Farquhar, G.D., 1981. Some relationship between the biochemistry of photosynthesis and the gas exchange of leaves. Planta 153, 376–387.

Vygodskaya, N.N., Gorshokova, I.I., 1989. Calculations of canopy spectral reflectances using the Goudriaan reflectance model and their experimental evaluation. Remote Sens. Environ. 27, 321–336.

Walcroft, A.S., Whitehead, D., Silvester, W.B., Kelliher, F.M., 1997a. The response of photosynthetic model parameters to temperature and nitrogen concentration in *Pinus radiata* D. Don. Plant Cell Environ. 20, 1338–1348.

Walcroft, A.S., Silvester, W.B., Whitehead, D., Kelliher, F.M., 1997b. Seasonal changes in stable carbon isotope ratios within annual rings of *Pinus radiata* reflect environmental regulation of growth processes. Aust. J. Plant Physiol. 24, 57–68.

Wang, Y.-P., Leuning, R., 1998. A two-leaf model for canopy conductance, photosynthesis and partitioning of available energy I: Model description and comparison with a multi-layered model. Agric. For. Meteorol. 91, 89–111.

Williams, M., Rastetter, E.B., Fernandes, D.N., Goulden, M.L., Wofsy, S.C., Shaver, G.R., et al., 1996. Modelling the soil-plant-atmosphere continuum in a *Quercus-Acer* stand at Harvard Forest: the regulation of stomatal conductance by light, nitrogen and soil/plant hydraulic properties. Plant Cell Environ. 19, 911–927.

Wohlfahrt, G., Cernusca, A., 1999a. Modelling leaf gas exchange. In: Cernusca, A., Tappeiner, U., Bayfield, N. (Eds.), Land-use Changes in European Mountain Ecosystems. ECOMONT — Concepts and Results, Blackwell Wissenschafts-Verlag, Berlin, pp. 188–191.

Wohlfahrt, G., Cernusca, A., 1999b. Scaling up gas exchange from leaves to single plants. In: Cernusca, A., Tappeiner, U., Bayfield, N. (Eds.), Land-use Changes in European Mountain Ecosystems. ECOMONT — Concepts and Results, Blackwell Wissenschafts-Verlag, Berlin, pp. 191–194.

Wohlfahrt, G., Bahn, M., Horak, I., Tappeiner, U., Cernusca, A., 1998. A nitrogen sensitive model of leaf carbon dioxide and water vapour gas exchange: application to 13 key species from differently managed mountain grassland ecosystems. Ecol. Model. 113, 179–199.

Wohlfahrt, G., Bahn, M., Haubner, E., Horak, I., Michaeler, W., Rottmar, K., et al., 1999. Inter-specific variation of the biochemical limitation to photosynthesis and related leaf traits of 30 species from mountain grassland differing in land use. Plant Cell Environ. 22, 1281–1296.

Wullschleger, S.D., 1993. Biochemical limitations to carbon assimilation in C_3 plants — a retrospective analysis of the A/Ci curves from 109 species. J. Exp. Bot. 44, 907–920.

Yang, S., Liu, X., Tyree, M.T., 1998. A model of stomatal conductance in sugar maple (*Acer saccharum* Marsh). J. Theor. Biol. 191, 197–211.

Yu, G.-R., Nakayama, K., Matsuoka, N., Kon, H., 1998. A combination model for estimating stomatal conductance of maize (*Zea mays* L.) leaves over the long term. Agric. For. Meteorol. 92, 9–28.